Response to Editor's Comments

We would like to sincerely thank the Executive Editor, Editor (Dr.Gabriele Stiller) and all the referees for kind suggestions and comments, which helped in revising the manuscript. We have addressed all the reviewers' comments in order to make the manuscript publishable in your esteemed journal "Atmospheric Chemistry and Physics (ACP)".

Point-by-point response on how we have addressed each recommendations/suggestions is given in the reply to the reviewer's comments and same is also implemented in the revised manuscript.

Now we are herewith submitting the following for the consideration of publication:

1. **Replies to the reviewer's comments (in .pdf)**
2. **Track change manuscript along with figures and tables (in .pdf)**
3. **Revised manuscript with figures and tables (in LaTex)**

All the authors listed on the manuscript concur with submission of the above mentioned manuscript.

We request Executive Editor and Editor to kindly process further and do the needful.

--END--

Response to Reviewer-1's comments

The authors have revised the manuscript reasonably in response to my first review. Below, I list several minor suggestions, which the authors may consider when they prepare the final manuscript. (The following line numbers refer to those in acp-2020-18-author_response-version2.pdf, i.e., the changes-tracked version.)

We would like to sincerely thank the referee-1 for the second evaluation and very positive and constructive suggestions and recommendation for publication. We have implemented the suggestions raised by the referee.

Point-by-point responses on how we have addressed each recommendation/ suggestions are given below.

Q1: *Lines 14: add ", India"*
R1: Corrected in the revised manuscript.

Q2: *Lines 15: add ", Indonesia"*
R2: Corrected in the revised manuscript.

Q3: *Lines 21-22: I think this sentence needs clarification. One possibility is ". . . in the w when testing different spatial sampling for reanalysis data around the Gadanki station."*
R3: Corrected in the revised manuscript.

Q4: *Line 168: add ", India" and ", Indonesia"*
R4: Added in the revised manuscript.

Q5: *Line 188, Table 1: add the information on the horizontal extent (in km or km^2) of the radar sampling volume at e.g., 10 km and 20 km altitudes.*
R5: The sampling volume is 0.85 km^2 at 10 km and 3.4 km^2 at 20 km.

Q6: *Line 214: Change "daily mean profiles" to "daily 16:30-17:30 IST (11:00-12:00 UTC) averaged profiles"*
R6: Changed in the revised manuscript.

Q7: *Line 254: "This wind shear" – add the information on the altitude*
R7: Added in the revised manuscript.

Q8: *Lines 255-256: Do you mean "above 6-7 km altitudes" ? If so, please explicitly write so.*
R8: Added in the revised manuscript.

Q9: *Line 415: "long-period" – please explicitly write the temporal scale.*
R9: It is from 1986 to 1989. Now added in the revised manuscript.

Q10: *Line 416: "long-term" – again, please explicitly write the temporal scale.*
R10: Gage et al. (1991) has taken three years of data and mentioned it as long-term mean. Corrected in the revised manuscript.

Q11: *Line 480: "long-term" – same as above. "diurnal" – is this "day-to-day"? ("diurnal" may mean 1-day (and 0.5-day) periodicity)*
R11: Corrected in the revised manuscript.

Q12: *Line 715: "any" – did you do the same analysis for other reanalyses? Or, only ERA-Interim?*
R12: Yes, it is true for all the re-analysis data. We have done the same analysis for all the re-analyses data and the results are consistence.

Q13: *Lines 717-718: Change this sentence to: "We therefore show the directional tendencies of reanalysis data relative to the radar measurements." Here, I assume that the authors use the term "tendencies" as the ratio that reanalysis reproduces (i.e., agree with) radar measurements in terms of vertical wind direction. Also, I think we need one more sentence, right after this, explaining/defining what is "directional tendencies" more clearly, or please add something like: "The directional tendencies would be 100% when all radar measurements at certain height range are reproduced by a reanalysis in terms of vertical wind direction."*
R13: Revised in the manuscript.

Q14: *Lines 726-951: All "produce/producing/produced" should be changed to "reproduce/reproducing/ reproduced".*
R14: Corrected in the revised manuscript.

Q15: *Line 1004: "any": again, did you do the same analysis for other reanalyses?*
R15: It will be true for all reanalyses. We have changed the sentences accordingly.

Q16: *Line 1010: change "care" to "caution"*
R16: Corrected in the revised manuscript.

Q17: *Figure 2, caption: change "MST Radar" to "IMSTR"*
R17: Corrected in the revised manuscript.

Q18: *Figure 4, caption: change "MST Radar" to "IMSTR"*
R18: Corrected in the revised manuscript.

Q19: *Figure 10, caption: add the following sentence (between the two sentences), "The reference is the reanalysis ensemble mean."*
R19: The figure caption is revised by following the reviewer's suggestion.

Q20: *Figure 12, caption: add the information that these are the ERAi cases.*
R20: The figure caption is revised.

Q21: *Table 2: Change "Kobayachi" to "Kobayashi". Also, commas after the author names are unnecessary if "(year)" is used.*
R21: Corrected in the revised manuscript.

--END--

Response to Reviewer-2's comments

Overall the manuscript provides a novel intercomparison of reanalysis vertical velocities with ground-based measurements from 2 subtropical VHF radar locations. The study illustrates how widely vertical velocities can vary among reanalyses and observations, meaning that caution should be used when interpreting results from studies using reanalysis-based vertical velocities in the troposphere and lower stratosphere.

We would like to sincerely thank anonymous referee-2 for the evaluation and providing constructive comments/suggestions, which helped to improve the manuscript considerably.

Point-by-point responses to the reviewer's comments are given below. Please note that changes are also made in the revised manuscript by taking consideration of referee #1s' comments.

Q1: *First, throughout the manuscript the authors should emphasize that this study focuses on a very limited geographical area, so the results do not necessarily apply for reanalyses in general. I think this is important, especially given the conclusion (lines 440-442) that the results somehow provide an initial basis to improve calculation of w in reanalyses. Instead, I would say that the results demonstrate that how approaches to generating global reanalysis products (encompassing different models, assimilation methods, spatial resolution, etc) can impact estimates of w. I think this is important since providing uncertainty estimates for derived meteorological products like w is currently needed by the SPARC community.*

R1: We do agree with the referee's assertion. Now we have re-written the concluding remarks in the revised manuscript.

Q2: *In that spirit, I think one thing that is currently missing from this paper, which is needed before I can recommend publication, is a quantitative discussion of the uncertainties in the retrieved vertical velocities from the radar. As other referees have commented, the authors do mention sources of uncertainty but I don't have an idea for what a typical error bar would be. For example, can the vertical velocities from an individual profile be determined with an accuracy of a cm/s or less? Perhaps this is described in other papers, but it needs to be discussed here so we can make sense of the comparisons with w from reanalyses, and perhaps also included in Table 1?*

R2: Following the reviewer's suggestion, we have provided a separate sub-section in the revised manuscript for accuracy and uncertainty in the measurements of *w* from. We request reviewer to kindly follow the revised manuscript for details. We thank referee for the suggestion.

We have also included the velocity resolution by EAR and IMSTR in Table 1.

Q3: *Another item that must be addressed is the process for computing vertical velocities from reanalyses on an altitude grid. Again, earlier referee comments requested clarification, particularly because vertical velocity is essentially a model-produced variable and so is subject to the details of each system (model vertical coordinate, vertical resolution especially in the TTL region, in addition to model physical parameterizations, etc). I only saw a brief mention in one of the author responses that the conversion to altitude is done using the hypsometric equation. Details are needed, and I'm not sure that is the best way to do things, if the authors are saying the performed some kind of integration themselves using temperature profiles to determine geometrical altitude (z). The most straightforward method would seem to be using the reanalysis Geopotential height fields to specify the altitude of each pressure level at each grid point where pressure velocity is evaluated. Can the authors please provide specific details about how geometric altitude conversion was performed. This could potentially clear up any underlying biases or disagreements among the observations and reanalyses w profiles.*

R3: Reanalysis gives the omega at different pressure levels. The pressure is converted to geometric altitude using the hypsometric equation which is

$$P=P_0\exp^{(-Z/H)} \quad (1)$$

where, P is the pressure at a particular altitude and P_0 is the surface pressure. Z is the height and H is the scale height.
After the pressure conversion to height, omega is converted into vertical velocity using the equation

$$W = -\frac{1}{g}\omega\frac{RT}{p} \tag{2}$$

Hence no integration or interpolation of omega is done.

Q4: *Finally, the manuscript does not mention that one very large source of observations in the troposphere and lower stratosphere come from radiosondes (in fact, a search of the manuscript finds no mention of radiosondes at all, which I find quite surprising). First, I believe radiosondes can provide vertical wind information that is directly assimilated into these analysis systems. I would assume there have been comparisons between the VHR radar vertical velocities and nearby radiosonde observations (a very brief search provides many results, including some early studies by some of the coauthors of the present manuscript). If so, these should be mentioned, and how do they compare? This would further support the validity of the radar observations and also further highlight possible issues with reanalyses (i.e, if they assimilate radiosonde vertical velocities and still giving different results, that's an issue).*

R4: There are few studies that have calculated vertical velocity from dropsondes and radiosondes. Wang et al. (2009) derived the vertical velocity from radiosonde and dropsondes, however the authors themselves have pointed out the several uncertainties like requirement of high resolution radiosonde data, amount of helium gas associated with such retrievals and accuracy of the estimated vertical velocity was not quantified. Zhang et al. (2019) estimated vertical velocity using a descending radiosonde system. Here also the authors have pointed out the uncertainties involved especially with the radiosonde descent speed, calculation of drag coefficient and also on the validation of the retrieval's on vertical velocity obtained. However, reanalysis does not assimilate the vertical velocity obtained from the radiosonde, it only derives the vertical wind using the horizontal wind divergence. The horizontal winds from the radiosonde are well assimilated in all the reanalysis system.
Now we have briefly discussed the above in the revised manuscript.

Q5: *Throughout the manuscript please use UTC consistently instead of UTS and GMT.*
R5: Corrected in the revised manuscript.

Q6: *Make sure all figure captions clearly indicate the time period of the results. This is missing from, e.g., caption of Figs. 4, 5, 8, 9, 10, 11, 12, 13.*
R6: Implemented in the revised manuscript.

Q7: *Lines 51-52: This statement clearly is not true for aircraft measurements. Please revise to more accurately capture what the relevant point is (e.g., that independent ground based observations are limited in their geographic distribution).*
R7: Modified in the revised manuscript.

Q8: *lines 89-91: Meteor radar is a technique for the mesosphere, and is not applicable in the present study, this should be removed.*
R8: Removed in the revised manuscript.

Q9: *The abstract and introduction should clearly state that this study is focusing on the troposphere and lower stratosphere. I had to read quite far into the manuscript to determine the scope of the study. Since this is submitted to the SRIP special issue, revisions that specifically address the relevance of this study to SRIP would be greatly beneficial.*

R9:Following the reviewer's suggestion we have modified the abstract and introduction in the revised manuscript. A brief description of SPARC/s-rip is provided also described.

Q10: *Lines 101-102 and elsewhere: Throughout the manuscript the authors use the term tendency to describe the sign of the vertical velocity (positive or negative). This is in opposition to the usage I am most familiar with, i.e., a time tendency, or specifically, a time derivative. I think it is better to say here that the best way (in the authors' opinion) is to evaluate time-mean profiles, which is what they are doing in figures 4, 5, 6, etc.*

R10: Following the reviewer-1's comment (Q13), we have includes a brief note on directional tendency in the revised manuscript.

References :

Wang, J., J. Bian, W. O. Brown, H. Cole, V. Grubisic and K. Young.: Vertical air motion from T-REX radiosonde and dropsonde data, J. atmos. Oce. Tech., 26, 928-942, https://doi:10.1175/2008JTECHA1240.1, 2009

Zhang, J., H. Chen, Y. Zhu, H. Shi, Y. Zheng, X. Xia, Y. Teng, F. Wang, X. Han, J. Li and Y. Xuan.: 2019, A novel method for estimating the vertical velocity of air with a descending radiosonde system, Rem. Sens., 11, 1538, https://doi:10.3390/rs11131538, 2019.

--END--

Assessment of vertical air motion among reanalyses and qualitative comparison with VHF radar measurements over the two tropical stations

K. N. Uma[1], Siddarth Shankar Das[1], M. Venkat Ratnam[2], and K. V. Suneeth[1,3]

[1]Space Physics Laboratory, Vikram Sarabhai Space Centre, ISRO, Trivandrum-695022, India
[2]National Atmospheric Research Laboratory, Dept. of Space, Gadanki-517112, India
[3]Numerical Weather Prediction Division, India Meteorological Department, MoES, New Delhi-110003, India

*e-mail : urmi_nmrf@yahoo.com

Abstract

Vertical wind (*w*) is one of the most important meteorological parameters for understanding a range of different atmospheric phenomena. Very few direct measurements of *w* are available so that most of the time one must depend on reanalysis products. In the present study, assessment of *w* among selected reanalyses, (ERAi, ERA5, MERRA-2, NCEP/DOE-2 and JRA-55) and qualitative comparison of those datasets with VHF radar measurements over the convectively active regions Gadanki (13.5°N and 79.2°E), India and Kototabang (0°S and 100.2°E), Indonesia are presented for the first time in the troposphere and lower stratosphere. The magnitude of *w* derived from reanalyses is 10-50% less than that from the radar observations. Radar measurements of *w* show downdrafts below 8 to 10 km and updrafts above 8-10 km over both locations. Inter-comparison between the ensemble of reanalyses with respect to individual reanalysis shows that ERAi, MERRA-2 and JRA-55 compares well with the ensemble compared to ERA5 and NCEP/DOE-2. There is no significant improvement in the *w* due to the effect of different spatial sampling for reanalysis data around the Gadanki station. Directional tendency shows that the percentage of updrafts captured is reasonably good, but downdrafts are not well captured by all reanalyses. Thus, caution is advised when using vertical velocities from reanalyses.

Key Words: Vertical velocity, MST Radar, Equatorial Atmosphere Radar, Reanalysis

Deleted: ¶

1 Introduction

Vertical air motion (*w*) in any region of the Earth's atmosphere reflects the structure and dynamical features of that region. Importantly, in the lower part of the atmosphere, sudden widespread changes in the weather are usually associated with variations in vertical air motion. The magnitude of *w* is a factor of ten or more smaller than the horizontal wind; nevertheless, it is crucial in the evolution of severe weather (Peterson and Balsley, 1979). Adiabatic cooling associated with upward motion leads to the formation of clouds and precipitation and adiabatic warming associated with downward motion leads to the dissipation of clouds. In addition, subsidence leads to adiabatic warming, which results in the formation of stable inversion layers. Extensive studies have been done on the relationships between *w* and precipitation/convection over the tropics (Back and Bretherton, 2009; Uma and Rao, 2009a; Rao et al., 2009; Uma et al., 2011 and references therein). Thus, *w* plays a vital role in day-to-day changes in the weather. Different scales of variability exist in *w* ranging from microscale to meso synoptic, and planetary - scales (Uma and Rao, 2009b). It also controls energy and mass transport between the upper troposphere and lower stratosphere (Yamamoto et al., 2007, Rao et al., 2008). In a nutshell, knowledge of *w* is helpful for evaluating virtually all physical processes in the atmosphere. Hence precise measurements of *w* could serve a guiding factor for studying many processes in the atmosphere.

The small magnitudes of *w* make it very difficult to measure, as the errors involved in measurements often exceed the actual values. Direct and indirect methods exist to measure *w* (e.g. Doppler measurements using radars for profiling, sonic anemometers in the boundary layer, radiosondes and also aircrafts) as well as indirect computational methods (e.g., adiabatic, kinematic and quasi-geostrophic vorticity/omega methods).

Deleted: ¶

Formatted: Font: (Default) Times New Roman, 12 pt, Bold, Font color: Text 1, Complex Script Font: Bold

Formatted: Font: Not Italic, Complex Script Font: Not Italic

Formatted: Font: Not Italic, Complex Script Font: Not Italic

Formatted: Font: Not Italic, Complex Script Font: Italic

Formatted: Complex Script Font: Italic

Formatted: Font: Not Italic, Complex Script Font: Not Italic

Formatted: Font: Not Italic, Complex Script Font: Not Italic

Formatted: Font: Not Italic

Deleted:

With respect to radiosondes, very few studies have calculated vertical velocity. Wang et al. (2009) derived the vertical velocity from radiosonde and dropsondes, however the authors pointed out several uncertainties like requirement of high resolution radiosonde data, amount of helium gas associated with such retrievals and, accuracy of the estimated vertical velocity was not quantified. Zhang et al. (2019) estimated vertical velocity using a descending radiosonde system. The authors pointed out the uncertainties involved especially with radiosonde descent speed, calculation of drag coefficient and also on the validation of the retrieval's on vertical velocity obtained. Using aircrafts Schumann, (2019) studied the relationships between horizontal kinetic energy spectra of vertical wind and horizontal divergence of the divergent horizontal wind components, by separating it from the rotational wind components by known Helmholtz decomposition methods. Radars provide the direct measurement of *w* and hence remote sensing measurements of *w* are thus restricted to locations where radars are situated.

In general, *w* is derived diagnostically from horizontal winds and temperatures, which is an indirect estimation. This estimation gives a general view on the distribution of ascending and descending motion on the synoptic-scale within the quasi-geostrophic framework (Tanaka and Yatagai, 2000; Rao et al., 2003). Reanalyses evaluate the vertical pressure velocity (omega) using indirect estimation (e.g., Dee et al., 2011). Any reanalyses products assimilate as much as 10^7 observations per day, which is inclusive of both conventional (radiosonde, tower, aircrafts, wind profilers (wherever possible), etc.) as well as various satellite observations. However, reanalyses combine both observations and model outputs to produce systematic variation in the atmospheric state (e.g., Fujiwara et al., 2017). It is to be noted that the vertical velocity provided by any reanalysis data center is estimated indirectly from the horizontal wind components and temperature, which itself has mismatch among various reanalyses data (e.g., Das et al., 2016; Kawatani et al., 2016). Thus, this can

Formatted: Font: Not Bold, Complex Script Font: Not Bold

Formatted: Font: Not Bold, Complex Script Font: Not Bold

Formatted: Font: Not Bold, Complex Script Font: Not Bold

Formatted: Font: Not Italic, Complex Script Font: Not Italic

Formatted: Font: Italic, Complex Script Font: Italic

Moved (insertion) [1]

Deleted: R

Deleted: as well as indirect computational methods (e.g., adiabatic, kinematic and quasi-geostrophic vorticity/omega methods). Remote sensing measurements of *w* are thus restricted to locations where radars are situated. Using aircrafts *Schumann*, (2019) studied the relationships between horizontal kinetic energy spectra of vertical wind and horizontal divergence of the divergent horizontal wind components, by separating it from the rotational wind components by known Helmholtz decomposition methods.

Moved up [1]: Remote sensing measurements of *w* are thus restricted to locations where radars are situated.

Formatted: Font: Not Italic, Complex Script Font: Not Italic

Formatted: Font: Not Italic, Complex Script Font: Not Italic

Deleted: ¶

Formatted: Font: Not Italic, Complex Script Font: Not Italic

Formatted: Font: Not Italic, Complex Script Font: Not Italic

Formatted: Font: Not Italic, Complex Script Font: Not Italic

Formatted: Font: Not Italic, Complex Script Font: Not Italic

possibly induce the discrepancy in the estimated vertical velocity among various reanalyses. For example, in the kinematic method, omega is estimated by integrating the mass continuity equation assuming inviscid adiabatic flow. However, this kinematic estimate suffers from uncertainties in the observations as omega is estimated from horizontal divergence (Tanaka and Yatagai, 2000). This source of uncertainty is particularly important for reanalyses, where assimilation increments in horizontal winds may be comparable to the uncertainty. A 10% error in the wind may lead to a 100% error in the estimated divergence (Holton, 2004). Omega from the thermodynamic energy equation is less sensitive to horizontal winds as it mainly depends on the temperature gradient. However, in this method the local rate of change in temperature must be measured accurately, meaning that observations must be taken at frequent intervals in time to estimate $\partial T / \partial t$ accurately (Holton, 2004). This methodology fails in areas of strong diabatic heating, especially where condensation and evaporation are involved. The quasi-geostrophic method for estimating omega neglects ageostrophic effects, friction and diabatic heating (Stepanyuk et al., 2017). It is to be noted from the above discussions that calculating *w* from indirect estimation has more uncertainties. Hence reanalyses that use indirect estimation, involve underlying approximations and assimilations and are not error-free (Kennedy et al., 2012). Other indirect methods can be used to derive *w* from radar measurements in the middle and upper atmosphere, where direct measurements of vertical wind are not possible due to technical constraints. These methods include Doppler weather radar, Medium Frequency (MF) radar and meteor radar. Doppler weather radar uses an indirect method to calculate vertical winds (Liou and Chang, 2009; Matejka, 2002).

Very-high frequency (VHF) and ultra-high frequency (UHF) vertical pointing radars are the most powerful tools for determining vertical air motion (velocity) with high temporal and vertical resolution. However, the magnitude may still not be directly comparable between reanalysis products and observations as the reanalyses provide the intensity of vertical air

Formatted: Font: Not Italic, Complex Script Font: Not Italic

Formatted: Font: Not Italic, Complex Script Font: Not Italic

Formatted: Font: Not Italic, Complex Script Font: Not Italic

Formatted: Font: Not Italic, Complex Script Font: Not Italic

Formatted: Font: Not Italic, Complex Script Font: Not Italic

Deleted: ¶

Formatted: Font: Not Italic, Complex Script Font: Not Italic

Deleted: Meteor radar also cannot determine vertical velocity directly as the winds are determined from meteor showers using a wide beamwidth. As a consequence, *Laskar et al*. (2017) calculated vertical wind from meteor wind radar data based on a "Kinematic" method using the continuity equation and hydrostatic balance. *Dowdy et al.* (2001) have calculated vertical wind using the horizontal momentum and mass continuity equations from the MF radar data. However, indirect methods are only adopted when direct methods cannot be used.

Formatted: Font: Not Italic, Complex Script Font: Not Italic

motion over wide areas (> 25 km^2), whereas the radar measurements provide information for a narrower column over a single location. Thus, the best way to assess reanalysis estimates of *w* against radar measurements is to compare its directional tendencies. A number of studies have evaluated vertical motion across reanalyses (in the context of trajectories, wave activity, large-scale motion, etc.), so the primary novelty of this work is the evaluation against radar observations.

Stratosphere–troposphere Processes And their Role in Climate (SPARC) has initiated an activity known as SPARC Reanalysis Intercomparison Project (S-RIP) (Fujiwara et al., 2013; Fujiwara and Jackson, 2013; Fujiwara et al., 2017). The main objectives of S-RIP are to evaluate different reanalysis products, their differences with respect to different measurements, and also to suggest improvement for better usage by the scientific community (http://s-rip.ees.hokudai.ac.jp). The present study hence focuses on the assessment of *w* in the troposphere and lower stratosphere among various reanalyses using VHF radar measurements from two tropical stations where the convective activity is frequent: Gadanki and Kototabang.

Moved down [6]: The present study focuses on the assessment of *w* in the troposphere and lower stratosphere among various reanalyses using VHF radar measurements from two tropical stations where the convective activity is frequent: Gadanki and Kototabang.

Moved (insertion) [6]

Deleted:

Evaluations of this type are critically important as reanalyses estimates of *w* are widely used by the scientific community to understand and simulate a variety of atmospheric processes. In section 2, the data and methodology are described. Section 3 provides results and discussion followed by summary and concluding remarks in section 4.

Deleted:

Formatted: Indent: First line: 0"

2 Data and Methodology

2.1 *Radar measurements*

Formatted: Font: (Default) Times New Roman, 12 pt, Bold, Font color: Text 1, Complex Script Font: Bold

Formatted: Font: (Default) Times New Roman, Bold, Italic, Font color: Text 1, Complex Script Font: Bold

Remote sensing measurements of *w* are obtained from the Indian Mesosphere-Stratosphere-Troposphere Radar (IMSTR) located at Gadanki (13.5^{o}N and 79.2^{o}E), India and the Equatorial Atmosphere Radar (EAR) located at Kototabang (0.2^{o}S and 100.2^{o}E), Indonesia. Figure 1a and 1b show the topography map of the location of both the radars, i.e.

Deleted:

Gadanki and Kototabang respectively, generated by using the Shuttle Radar Topography Mission (SRTM) data (Farr et al., 2007). Gadanki is located in the southern peninsula of tropical India, about 90 km off the east coast and it is surrounded by hills. Kototabang is located in the western part of Sumatra Island and EAR is situated in the mountainous region with the highest peak of about 2 km. Both the IMSTR and EAR are pulsed coherent radars operating at 53 MHz and 47 MHz, respectively. These instruments are used to estimate *w* by measuring the Doppler shift in the vertical beam. The technical details and operational parameters of the IMSTR have been given by Rao et al. (1995) while those for the EAR have been given by Fukao et al. (2003). Both the radars specifications, parameters including velocity resolution used for the present measurements are listed in Table 1.

In the present study measurements of *w* from VHF radars are used to assess vertical motion between the surface and the lower stratosphere. Data collected from the IMSTR between 17:30 and 18:30 LT (LT=UTC+5:30 hr) from 1995 to 2015 are analyzed using the adaptive method (Anandan et al., 2001). This is the common operational mode of the IMSTR for deriving the winds and represents the only data available for such a long period of time. The three components of wind : zonal, meridional and vertical can be computed with the radial velocity obtained in atleast 3 non-coplanar directions. However, for the present analysis we have computed the *w* directly only using the vertical beam using equation (1)

$$w = -\frac{\lambda}{2} f_d, \quad (1)$$

Where, λ is the radar wavelength (in cm) and f_d is the Doppler velocity (Hz).

In general, 4-8 vertical profiles are averaged to create daily 16:30-17:30 IST (11:00-12:00 UTC) averaged profiles. Averaging is conducted using the arithmetic mean as it represents the central tendency, which is generally used for wind averaging. In a vertically pointing beam, signal-to-noise ratio (SNR) decreases with height except in stable layers (like the tropopause) and in the presence of strong turbulence. Above 25 km, the SNR becomes

Formatted: Font: Not Italic, Complex Script Font: Not Italic

Formatted: Font: Not Italic, Complex Script Font: Not Italic

Deleted: and

Formatted: Font: Not Italic, Complex Script Font: Not Italic

Formatted: Indent: First line: 0.31"

Deleted: GMT

Formatted: Font: Not Italic, Complex Script Font: Not Italic

Deleted: mean profiles

Formatted: Font: Bold, Complex Script Font: Bold constant in the absence of atmospheric signals. Data in this region can be therefore treated as noise and used to estimate the threshold SNR (Uma and Rao, 2009b). Noise levels estimated in this way lie between -17 dB and -19 dB with a 2σ value of 3 dB (where σ is the standard deviation). Thus data having SNR less than -15 dB are discarded from the present analysis. Data from intense convective days (checked for individual profiles), defined as *w* being less/greater than ± 1 ms^{-1} are also discarded as these data severely bias the climatological mean vertical velocity (e.g. Uma and Rao, 2009b). The data discarded is less than 1 % of the total data. Quality control metadata for the EAR measurements are available online (http://www.rish.kyoto-u.ac.jp/ear/data/index.html). The EAR operates continuously and this study uses hourly data (diurnal data of single day) of *w* computed using the vertical beam (equation (1)) from 2001 to 2015. The EAR data during convective periods are eliminated following the same criteria as for the IMSTR, a second screening step. Each full diurnal cycle (after removing convective profiles) is averaged and considered as a single daily profile for the EAR.

2.2 Accuracy and uncertainty in the w measured from Radar

The assumption in the radar measurements of wind components is the spatial homogeneity in the given time frame, when we used 3 non-coplanar beams (e.g., two off-zenith and one vertical). Thus, to avoid the bias, we use only vertical beam (equation (1)) for the direct estimation of *w*. which also provides a better time-resolution (Peterson and Balsley, 1979; Koscielny et al., 1984). The accuracy of the *w* measured made using the vertical beam of VHF radar depends on the alignment of the beam along the zenith direction. Any error in the beam pointing would mean that the line-of-sight velocity measured by the radar will have a component of the horizontal wind (Hauman and Balsley,1996). The beam pointing error is found to be ±0.2^{o} off-zenith, which was provided by calibrating the beam pointing with a known radio source Virgo-A (Damle et al. 1991; Rao et al. 1995) and Cygnus-A for EAR

Formatted: Font: Not Italic, Complex Script Font: Not Italic

Formatted: Font: Not Italic, Complex Script Font: Not Italic

Formatted: Font: Not Italic, Complex Script Font: Not Italic

Deleted: For both radars, vertical velocity (cm s^{-1}) is directly estimated using equation (1)¶
$w = -\frac{\lambda}{2} f_d$, (1)¶
where λ is the radar wavelength (in cm) and f_d is the Doppler velocity (Hz).

Formatted: Font color: Text 1

Formatted: Font color: Text 1

Formatted: Font color: Text 1

Formatted: Font: (Default) Times New Roman, Bold, Italic, Font color: Text 1, Complex Script Font: Bold

Formatted: Indent: First line: 0.31"

Moved (insertion) [3]

Deleted: The resolution of velocity using IMSTR is about 0.03 m s^{-1} if FFT points are 256, Coherent integration is 64 and inter-pulse period is 1000 μ s^{-1} and about 0.002 m s^{-1} if FFT points are 256, Coherent integration is 512 and inter-pulse period is 1000 μ s^{-1}. ¶

Formatted: Font: Italic, Complex Script Font: Italic

Formatted: Font: Not Italic, Complex Script Font: Not Italic

Moved (insertion) [2]

Deleted: the

(Fukao et al., 2003). The uncertainty in the *w* due to beam pointing error by an angle (*θ*) with a horizontal wind (*u*) is given by (*u*.sin *θ*). Thus, with a horizontal wind of 10 m s^{-1} and beam pointing error of 0.2 degree turns out to be 0.03 m s^{-1} uncertainty in the *w* measured from VHF radar. The beam pointing accuracy can further be determined by comparing the vertical wind obtained using two orthogonal polarizations, i.e., east-west and north-south polarizations, which are phased independently. Significant correlation was observed between both the polarizations, suggesting that the radar measures the true vertical velocity (Viswanathan et al. 1993. In addition, Rao et al. (2008) also estimated the vertical velocities from zenith beam and compared it with those estimated from 10-degree off-zenith beams using IMSTR. The differences were observed to be meager, which shows that the error due to beam pointing is negligible.

Tilting of reflecting layers contributing to the diffuse reflection can also adversely bias in the mean *w* (Röttger, 1980). These tilting layers can be due to the presence of Kelvin-Helmholtz instabilities(Muschinski, 1996), gravity waves, which includes inertia-gravity waves and mountain waves and causes imbalance in the echo power between the two polarizations in the same plane (Yamamoto et al. 2003). Rao et al. (2008) estimated the echo power imbalance in the east-west and north-south polarizations for both EAR and IMSTR and found the difference to be within ±1 dB, statistically indicating the bias due to the tilting layers is negligible over both the locations.

Nastrom and VanZandt (1994) proposed that *w* can be biased by gravity waves. Thus, Rao et al. (2008) have investigated the biases caused by gravity waves by calculating the variances and found that downward wind measurements below 10 km are essentially unaffected by gravity waves. It is also to be noted that the topography over the two locations can generate mountain waves, if strong low-level winds are prevailing. Strong low-level winds are prevalent over Gadanki only from June to August and during these months, there is

Formatted: Font: Italic, Complex Script Font: Italic
Deleted: The error caused
Formatted: Font: Italic, Complex Script Font: Italic
Deleted: by the beam pointing, due to the uncertainty in the
Formatted ...
Deleted: of
Formatted ...
Deleted: using the relation¶
Formatted ...
Deleted: in
Formatted ...
Deleted: polarization with that of vertical wind ...
Formatted ...
Deleted: The correlation was observed to be hig ...
Deleted: ed that
Formatted ...
Formatted ...
Formatted ...
Formatted ...
Deleted:). The authors found a difference < 0.1 ...
Moved (insertion) [4]
Deleted: vertical…enith beams using IMSTR. T ...
Moved up [3]: The resolution of velocity using ...
Formatted ...
Formatted ...
Formatted ...
Moved (insertion) [5]
Deleted: As proposed by
Formatted: Indent: First line: 0.4"
Formatted ...
Deleted: *on the*
Formatted ...
Deleted: caused …y gravity waves, ...
Formatted ...
Deleted: It is known that estimates of *w* derived ...
Formatted: Font color: Text 1
Moved up [2]: The beam pointing error is four ...
Formatted ...
Deleted: ¶
Formatted: Font color: Text 1
Deleted: ¶ ...
Formatted ...
Moved up [4]: Rao et al. (2008) estimated the ...
Formatted ...

a critical level existing between 6 and 7 km due to the presence of strong wind shear, which will not support the propagation of mountain waves to higher altitudes. This wind shear between 6 and 7 km exists throughout the year over Kototabang. Hence the effect of mountain waves will be minimal over both these locations on vertical velocity. Their analysis clearly showed that the mean downward motion below 10 km and upward motion above 10 km are real and not caused by measurement biases, and also that the known biases do not change the direction of the background *w* when measurements are averaged over longer periods of 10 years.

2.3 *ERA-Interim (ERAi)*

ERAi is global reanalyses data which is developed by European Centre for Medium-Range Weather Forecasts (ECMWF). The data assimilation scheme used is 4D-Var of the upper-air atmospheric state and have effectively anchored both satellite and in-situ observations. This scheme updates parameters that define bias corrections required for satellite observations. The model has improved in the representation of moist physical processes. Advances have also been made with respect to soil hydrology and snow in land surface models. The detail of the model is given in (Dee et al., 2011). We use 6-hourly vertical velocities from the ECMWF Interim reanalysis (ERAi) from 1995 to 2015. The grid resolution of ERAi is 0.75^{o} (latitude) x 0.75^{o} (longitude). The nearest grid points are taken for Gadanki (13.68^{o} N, 79.45^{o} E) and Kototabang (0.35^{o} S, 100.54^{o} E). Although 37 pressure levels up to 1 hPa resolution are available, we have restricted the dataset to 21 km, which is about 50 hPa, as that is the maximum radar range.

2.4 *ERA5*

ERA fifth-generation (ERA5) is the atmospheric reanalysis produced by ECMWF. It is an improved version of ERAi. The data assimilation scheme used is 4D-Var and it assimilates the NCEP stage IV quantitative precipitation estimates produced over the USA by combining

Moved up [5]: As proposed by *Nastrom and VanZandt* (1994) on the bias caused by gravity waves, *Rao et al.* (2008) have investigated biases caused by gravity waves by calculating the variances and found that downward wind measurements below 10 km are essentially unaffected by gravity waves.

Deleted: They found that the bias due to the gravity waves was found to be 0.1 cm s^{-1} which is less than mean w

Deleted:

Formatted: Font: (Default) Times New Roman, Bold, Italic, Font color: Text 1, Complex Script Font: Bold

Formatted: Font: (Default) Times New Roman, Bold, Italic, Complex Script Font: Bold

Formatted: Font: Not Italic, Complex Script Font: Not Italic

Formatted: Font: Not Italic, Complex Script Font: Not Italic

Formatted: Font: (Default) Times New Roman, Bold, Italic, Font color: Text 1, Complex Script Font: Bold precipitation estimates from the Next-Generation Radar (NEXRAD) network with gauge measurements. The moist physics scheme is improved by including freezing rain. The long wave radiation scheme is modified in ERA5. The evolution of the top soil layer, snow and sea ice temperatures are included. It uses observations from various satellites which include upper air temperature, humidity and ozone. It also used bending angles from GNSS. It provides much higher spatial (30 km) and temporal resolution (hourly) from the surface up to 80 km (137 levels). ERA5 also features much improved representation especially over the tropical regions of the troposphere and better global balance of precipitation and evaporation. Many new data types not assimilated in ERAi are ingested in ERA5 (Hoffmann et al., 2019). The grid resolution of ERA5 is 0.28^{o} (latitude) x 0.28^{o} (longitude). The details are available in (Hersbach et al., 2020). We have taken hourly data from ERA5. The nearest grid points are again taken for Gadanki (13.63^{o}N, 79.31^{o}E) and Kototabang (0.14^{o}S, 100.40^{o}E), and the data period is 2002-2015.

2.5 ***MERRA-2***

The Modern-Era Retrospective analysis for Research and Applications, version 2 (MERRA-2) is the latest reanalysis of the modern satellite era produced by the National Aeronautics and Space Administration's (NASA) Global Modelling and Assimilation Office (GMAO). The scheme used in MERRA-2 is an improved version of MERRA. It uses a three-dimensional variational (3D-Var) algorithm based on the grid point statistical interpolation and also uses an incremental analysis update. It assimilates bending angle observations, satellite radiances from both polar as well as geostationary infra-red and microwave sounders. In addition it also assimilates water vapor and ozone. MERRA-2 includes aerosol analysis and provide data for 42 pressure levels from the surface to 0.01 hPa with a temporal resolution of 3 h and horizontal resolution of 0.5^{o} (latitude)x 0.625^{o} (longitude). We used MERRA-2 Assimilation (ASM) data. Details have been provided by Gelaro et al. (2017). The

Formatted: Font: Not Italic, Complex Script Font: Not Italic

Formatted: Font: Not Italic, Complex Script Font: Not Italic

Formatted: Font: (Default) Times New Roman, Bold, Italic, Font color: Text 1, Complex Script Font: Bold

Formatted: Font: (Default) Times New Roman, 12 pt, Font color: Black, Complex Script Font: Times New Roman, 12 pt

Formatted: Font: (Default) Times New Roman, 12 pt, Not Italic, Font color: Black, Complex Script Font: Times New Roman, 12 pt, Not Italic

Formatted: Font: (Default) Times New Roman, 12 pt, Font color: Black, Complex Script Font: Times New Roman, 12 pt nearest grid points are used for Gadanki (13.5° N, 79.37° E) and Kototabang (0.14° S, 100.00° E), with data spanning from 1995 to 2015.

2.6 *NCEP/DOE-2*

The National Center for Atmospheric Research and Department of Energy (NCEP/DOE-2) reanalysis is an updated version of NCEP-1 by fixing the known processing errors in NCEP-1. The variational scheme used is 3D-Var and it provides more accurate pictures of soil wetness and near-surface temperature over land, the land surface hydrology budget, snow cover, and radiation fluxes over the ocean. It is based on the NCEP operational model with a horizontal resolution of 209 km and 28 vertical levels. The temporal coverage is four times per day. NCEP/DOE-2 products are improved relative to NCEP-1, having fixed errors and updated parameterizations of physical processes, as evaluated by Kanamitsu et al. (2002). The grid resolution of NCEP/DOE-2 is 2.5° (latitude) x 2.5° (longitude). The data for the present study covers from 1995 to 2015 and is extracted at the nearest grid points to Gadanki (12.5° N, 77.5° E) and Kototabang (0, 100.00° E).

2.7 *JRA-55*

The Japanese 55-year reanalysis (JRA-55) is an updated version of the earlier JRA-25 with new data assimilation and prediction systems (Kobayashi et al., 2015). New radiation schemes, higher spatial resolution and 4D-var data assimilation with variational bias correction for satellite radiances have been used to generate the JRA-55 products. This reanalysis includes variation in greenhouse gas concentrations with time, as well as the new representations of land surface parameters, aerosols, ozone and sea surface temperature. The grid resolution of JRA-55 is 1.25° (latitude) x 1.25° (longitude). The nearest grid points are taken for Gadanki (13.75° N, 78.75° E) and Kototabang (0, 100° E) and the data period is 1995-2015.

For all the reanalyses data, w (in cm s^{-1}) is estimated using the formula :

Formatted: Font: (Default) Times New Roman, 12 pt, Font color: Black, Complex Script Font: Times New Roman, 12 pt

Formatted: Font: (Default) Times New Roman, 12 pt, Font color: Black, Complex Script Font: Times New Roman, 12 pt

Formatted: Font: (Default) Times New Roman, 12 pt, Font color: Black, Complex Script Font: Times New Roman, 12 pt

Formatted: Font: (Default) Times New Roman, 12 pt, Font color: Black, Complex Script Font: Times New Roman, 12 pt

Deleted: spanning from

Formatted: Font: (Default) Times New Roman, 12 pt, Font color: Black, Complex Script Font: Times New Roman, 12 pt

Formatted: Font: (Default) Times New Roman, Bold, Italic, Font color: Text 1, Complex Script Font: Bold

Formatted: Font: Not Italic, Complex Script Font: Not Italic

Formatted: Font: Not Italic, Complex Script Font: Not Italic

Formatted: Font: (Default) Times New Roman, Bold, Italic, Font color: Text 1, Complex Script Font: Bold

Formatted: Font: Not Italic, Complex Script Font: Not Italic

$$w = -\frac{1}{g}\omega\frac{RT}{p} \tag{2}$$

where ω is the vertical velocity in pressure coordinates (in Pa s^{-1}), T is the absolute temperature (K), p is the atmospheric pressure (hPa) and R (=287 J kg^{-1} K^{-1}) is the gas constant for dry air. To compare measured vertical wind with the reanalysis products, we take the reanalysis data corresponding to 12 UTC for Gadanki and the daily mean for Kototabang. The details of the schemes used in reanalysis are provided in Table 2.

3 Results and Discussion

Figure 2 shows the inter-comparison of layer averaged daily *w* measured from IMSTR with different reanalyses (ERAi, ERA5, MERRA-2, NCEP/DOE-2, and JRA-55) over Gadanki for (a) January 2007, and (b) August 2007. Both radar and all the reanalyses data sets are taken at 12 UTC, and the month and year are chosen in such a way to have maximum days of radar observations in two different seasons (winter and summer). Similarly, EAR observation is also compared with different reanalysis data but for January 2008 and August 2008 as shown in Fig.3. However, both EAR and reanalysis data are diurnal averaged (24 hrs). It is observed that the magnitude of *w* measured from radar observations is an order higher than the reanalysis data over both the locations (Gadanki and Kototabang). Most of the time, reanalysis data are comparable in direction with radar observations, whenever updrafts are observed. It is also observed that there is mismatch between the *w* estimated in the different reanalyses. Gage et al. (1992) described that by averaging radar data for a long-period of time can give a better measurement of *w* in clear-air condition and the authors have used three years data to arrive at the above conclusion. Thus in this context, we have taken 20 years of data for averaging.

Figure 4 shows the climatological monthly mean altitude profile of *w* obtained from the IMSTR (observations) and the ERAi, ERA5, MERRA-2, NCEP/DOE-2 and JRA-55 reanalysis data over Gadanki. Although the magnitudes are of the same order between the

Deleted: GMT

Formatted: Font: (Default) Times New Roman, 12 pt, Bold, Font color: Text 1, Complex Script Font: Bold

Deleted: i

Deleted:) over

Formatted: Font: Not Italic, Complex Script Font: Not Italic

Deleted: and t

Deleted: long-term

Formatted: Highlight

Deleted:

observations and reanalyses, significant differences are identified in the figures. Convective days are discarded from the radar data (observations) as mentioned in the previous section and those days are also eliminated from all reanalysis data sets. The quantitative differences may be attributed to the spatial averaging implicit in the reanalyses products, whereas the radar measurements are for a single point. Thus we only discuss the tendency of *w* as it is used to represent the variation of *w*, rather than its magnitude. The IMSTR observations show updrafts between 8 and 20 km from December to April, with the largest values in the tropical tropopause layer (TTL, 12-16 km), These features are not reproduced by any of the reanalyses, which all show downdrafts from December to April between 1 km and the tropopause level (mean tropopause is ~ 16.5 km). By comparison, downdrafts are observed in the IMSTR below 6 km in April, which may be attributed to pre-monsoon (March-May) precipitation and evaporation (Uma and Rao, 2009a). Vertical velocity in ERAi differs in both magnitude and direction from other reanalyses, especially in the lower troposphere from March to June. Meanwhile, the magnitude of vertical velocity in ERA5 is a little larger than that in the other reanalyses from May to June. Updrafts are observed in the TTL by the IMSTR during June, when all reanalyses show similar features but only located below the TTL. During July and August both the radar observations and the reanalyses show updrafts in the vicinity of the TTL. Updrafts are observed in the TTL from September to November but the peak in the updrafts is shifted lower than that observed by the IMSTR. Below 8 km, the IMSTR shows downdrafts from April to October. The reanalyses data are unable to reproduce downdrafts above 2 km.

We have also analyzed *w* from the EAR (Kototabang) where the observations are available for the full diurnal cycle (measurements of hourly averages for 24 hrs of observations). All reanalyses data over Kototabang are averaged for the full diurnal cycle. Figure 5 shows the monthly mean climatology of daily mean *w* from the EAR observations

Formatted: Font: Not Italic, Complex Script Font: Not Italic

and the five reanalyses over Kototabang. All the reanalyses agree well with each other over Kototabang. The updrafts in the TTL are well reproduced by all five reanalyses although the magnitude and vertical location of the maximum in *w* remain lower than observed. However none of the reanalyses reproduces the downdrafts. A distinct bimodal distribution in *w* from May to September (two peaks between 8-10 km and 14-17 km) with a local minimum between 12 and 13 km is observed in the EAR measurements which are not observed in the reanalysis. The magnitudes of both updrafts and downdrafts are larger than those observed over Gadanki. JRA-55 produces the largest *w* among the reanalyses. The monthly means show significant differences in the direction of *w* between the observations and the reanalyses below 6 km.

Gage et al. (1992) studied the long-term diurnal variability of *w* at Christmas Island (2^{o}N) and found the *w* varies between ±4 cm s^{-1}. The observations showed updrafts below 4 km, downdrafts between 4-14 km and updrafts above 12 km. Gage et al. (1991) have explained that the downward motion in the troposphere is consistent with a heat balance in the clear-air between adiabatic warming of descending air and radiative cooling to space. The ascending motion in the upper troposphere and lower stratosphere is due to large diabatic heating caused by ice particle in the cirrus. Rao et al. (2008) have shown the long-term (11 years) mean of *w* over Gadanki and Kototabang and found *w* varies between -0.3 to +0.6 cm s^{-1}. The authors observed downdrafts below 6 km and updrafts above it in all the seasons. The mean pattern of *w* profile observed by radars over all the tropical sites (i.e. Christmas Island, Gadanki and Kototabang) show similar characteristics and explain that the vertical transport of air from the troposphere to the lower stratosphere is a two-step process as discussed by Rao et al. (2008). Uma and Rao (2009b) have reported the diurnal variation (using hourly data) of *w* in different seasons, although their observations had only 1-2 diurnal cycles per month over Gadanki. They found significant variations in the seasonal variability of diurnal

Deleted: is

Formatted: Font: Not Italic, Complex Script Font: Not Italic

Formatted: Font: Not Italic, Complex Script Font: Not Italic

Formatted: Font: Not Italic, Complex Script Font: Not Italic

Formatted: Font: Not Italic, Complex Script Font: Not Italic

Formatted: Font: Not Italic, Complex Script Font: Not Italic

cycle as large as ±6 cm s^{-1} over Gadanki using IMSTR. The present observations are limited to 16:30 to 17:30 IST, with all reanalyses data over Gadanki taken at 12 UTC (17:30 IST). Thus, time-averaged climatological mean biases can be neglected.

To establish the robustness of the results we have used different averaging procedures to assess the consistency of the variability in *w* at monthly scales. Monthly mean climatological profiles of *w* from radar observations and various reanalyses over Gadanki and Kototabang are shown in Figure S1 (supplementary). Downdrafts in the troposphere are not captured by any of the reanalyses over either location. By contrast, updrafts in the TTL are generally reproduced in the monthly mean, though their magnitudes are often underestimated by the reanalyses. ERAi underestimates the magnitude of both updrafts and downdrafts over Gadanki, while NCEP/DOE-2 underestimates the magnitude of updrafts over Kototabang.

Monthly means calculated over five-year periods from both the radar data and ERAi are shown in Figure 6 for Gadanki and Figure 7 for Kototabang. The reanalysis shows similar behavior to the overall climatology in each five-year average. The overall patterns of updrafts and downdrafts in the radar measurements of vertical velocity are also similar, indicating a consistent performance of the radar over the full 20 year analysis period.

To further elucidate potential biases in the results due to averaging, we have taken ERA5 at 12 UTC and compared it to the daily mean (obtained by averaging *w* at different times of the day) to show that the sampling restrictions at Gadanki do not bias the results obtained. Figures 8 and 9 show the mean *w* obtained at 12 UTC and also the mean obtained by averaging hourly analyses for each day for Gadanki and Kototabang, respectively. ERA5 is chosen for this evaluation as the data are available at one-hour intervals. The analysis shows some differences in the magnitude of *w*, with 12 UTC generally showing larger magnitudes compared to the daily means over Gadanki (although no such systematic differences are observed in Kototabang). The directional tendencies are also similar in both the profiles at both locations. This analysis shows that the results are not biased by taking data only at 12 UTC over Gadanki.

Our analysis to this point shows the level of consistency between the features observed by the radar and those in the reanalysis. To further understand the relative differences among the reanalyses we perform a monthly mean comparative analysis among the reanalyses, as shown in Figures 10 and 11 for Gadanki and Kototabang, respectively. We take an ensemble mean of all the five reanalyses and then subtracted the ensemble mean from each reanalysis. The differences are less than ±0.5 cm s^{-1} during December-January-February (DJF, winter). During MAM, the difference between the ensemble and reanalysis show ±2 cm s^{-1} below 5 km. Below 5 km NCEP/DOE-2 and ERAi is less, whereas ERA5, Merra-2 and JRA-55 are more than the ensemble. The difference above 6 km is less than ±0.5 cm s^{-1} above 6 km. JRA-55 shows a good comparison with the ensemble and above 10 km all the reanalyses the differences are minimal with the ensemble. During the monsoon (JJA), the difference is comparatively high in June compared to July and August. NCEP/DOE-2 and ERA5 are more and other reanalyses are less than the ensemble, however during July and August NCEP/DOE-2 it is less in the upper troposphere (10-18 km). Merra-2 and ERAi shows a good comparison with respect to the ensemble during July and August, JRA-55 also shows a good comparison in addition to Merra-2 and ERAi. During SON, the differences are comparatively less than MAM and JJA. The difference is less than ±0.5 cm s^{-1} during October and November except in September between 10 and 15 km where ERA5 and Merra-2 are more and ERAi and NCEP/DOE-2 are less than the ensemble. In general, ERA5 and NCEP/DOE-2 shows considerably more difference with the ensemble and other reanalyses (ERAi, Merra-2 and JRA-55) compare well with the ensemble.

Over Kototabang (Figure 11), it is interesting to note the difference between the ensemble and different reanalyses show a consistent pattern during all the months. JRA-55

Deleted: ,

and ERAi show good comparison with the ensemble, as the differences are less than ±0.2 cm s^{-1} in all the seasons, except in November where it exceeds ±0.5 cm s^{-1} in the lower and middle troposphere. Merra-2 is more and NCEP/DOE-2 is less than the ensemble at all the height regions. ERA5 is less below 10 km and more above with respect to the ensemble.

There may be some probable reasons for the differences in the vertical velocity measured by observations and those retrieved from reanalysis. The main bias in *w* might occur in the reanalysis due to the following (1) Indirect estimation of omega, (2) local topography influence in the reanalysis, (3) use of different schemes in the boundary layer, (4) interactions between subgrid physical parameterizations and the large-scale flow and (5) spatial and temporal sampling. However, it is difficult to address the above issues other than the spatial and temporal sampling. To elucidate the spatial-temporal averaging on the vertical velocity we have chosen different grid resolutions with Gadanki as a centroid and the map is shown in Fig. 12a. G1 to G5 represent different grid resolutions, varying from 0.7° to 5°. The data chosen is for January and July 2007 from ERAi. The height profile of *w* at different grid resolution and time is shown in Fig. 12b for January and in Fig.12c for July. It is observed that the grid resolution does not have any influence on the *w*. However, a significant change is observed between 00 and 12 UTC in the month of January which affected the diurnal mean in *w* (shown in the last panel). The same is not reflected in the month of July. The result shows that the narrowing down the reanalysis data spatially (reducing the horizontal sampling) will not improve the retrieval of *w* in any reanalyses.

The direction of *w* is an essential metric for comparing the reanalysis with the observations. We therefore show the directional tendencies of reanalysis data relative to the radar measurements. The directional tendencies would be 100% when all radar measurements at certain height range are reproduced by a reanalysis in terms of vertical wind direction. Figure 13a shows the directional tendencies based on the IMSTR and the reanalyses over

Deleted: We therefore show the directional tendencies from the IMSTR and the EAR measurements relative to those from the reanalysis data

Gadanki, while Figure 13b shows the directional tendencies based on the EAR and the reanalyses over Kototabang. The directional tendency is calculated at each height for every month when the radar or reanalysis data exceed 0.1 cms^{-1} in either directions. The directional tendency for each month is estimated and then aggregated into seasons. These directional tendencies are given in terms of percentage of occurrence with respect to height. The tendency is calculated separately for updrafts and downdrafts.

Over Gadanki during DJF all reanalyses produce updrafts (simultaneously by both radar and reanalysis) less than 10% of the time throughout the profile. During MAM these ratios increase to around 15%, with NCEP/DOE-2 reproducing updrafts about 25% of the time. During JJA and SON, the percentage occurrence increases with the height from 25% to a maximum of 50% between 12 and 14 km. The percentage occurrence of updraft then decreases from 14 to 20 km. This tendency trend is similar for all reanalyses. The maximum ratio of updrafts over Gadanki is located between 12 and 15 km altitude. The percentage occurrence of downdrafts over Gadanki is also less than 50% at all levels. During DJF and MAM the reanalyses reproduce downdrafts 40 to 50% of the time, a much higher frequency than that for updrafts (<10%). This fraction decreases above 10 km. By contrast, the percentage of downdrafts reproduced during JJA and SON is less than that of updrafts, with frequencies less than 25% at all levels during these seasons.

Over Kototabang the percentage occurrence of updrafts increases with height in all seasons reaching a maximum of 75- 90% between 10 and 14 km. Above 14 km the percentage decreases to a minimum of 5% at 19 km. Updrafts are rarely reproduced by the reanalyses altitudes less than 4 km. It is important to note that none of the reanalyses reproduce daily mean downdrafts exceeding 1 cm s^{-1} except ERAi and ERA5 which reproduced downdrafts below 6 km. The percentage of downdrafts increases above 17 km

Deleted: direction

Deleted: producing

Deleted: produce

Deleted: produce

Deleted: produce

Deleted: produce

Deleted: produce

where it reaches a maximum and show occurrence frequencies around 65 to 75% above 18 km.

4 Summary and concluding remarks

The present study assesses the vertical motion (*w*) in reanalyses against radar observations in the troposphere and lower stratosphere from the convectively active regions Gadanki and Kototabang. The assessment is carried out for five different reanalyses: ERAi, ERA5, MERRA-2, NCEP/DOE-2 and JRA-55. Measurements were collected using VHF radar at both locations. We have used 20 years of data from Gadanki and 17 years of data from Kototabang. The following points summarize the results of this unique study

1. The magnitude of *w* obtained from reanalyses is underestimated by 10-50% relative to the radar observations.
2. Observations over Gadanki showed updrafts from 8 to 20 km year around. All the reanalyses only reproduced this feature during JJA and SON when magnitudes were larger than 0.5 cm s^{-1} in the reanalyses data. However, the vertical location of the updrafts differs between the observations and the reanalyses. Downdrafts below 8 km are not captured well by reanalyses data.
3. Over Kototabang, all five reanalyses did not consistently reproduce downdrafts below 8 km in all months. Updrafts in the UTLS are captured well; however, the peak in the vertical distribution of *w* is different as over Gadanki.
4. Inter-comparison between the ensemble and each reanalysis data shows the ERAi, MERRA-2 and JRA-55 compares well with the ensemble compared to ERA5 and NCEP/DOE-2. Analysis also showed that the reduction in spatial sampling in all the reanalyses data does not have significant improvement in the magnitude *w*.
5. Assessment of directional tendencies show that updrafts are reproduced reasonably well in all five reanalyses data but downdrafts are not reproduced at all.

Deleted:

Formatted: Font: (Default) Times New Roman, 12 pt, Bold, Font color: Text 1, Complex Script Font: Bold

Deleted: any

Deleted: ERAi reanalysis

Deleted: magnitude *w*

Formatted: Font: Italic, Complex Script Font: Italic

Deleted: which may be true for other reanalyses also

Formatted: Font: Not Italic, Complex Script Font: Not Italic

Deleted: .

The present analysis reveals that downdrafts are not well captured in all the five reanalyses data. The location of the largest updrafts is also shifted lower in reanalyses than in the observations. It is to be noted that *w* measured from radar is limited over a geographical area and thus the results may be valid to a limited region. However, the results demonstrate that how approaches to generating global reanalysis products (encompassing different models, assimilation methods, spatial resolution, etc.) can impact estimates of *w*. Hence, reanalysis data should be used with caution for representing various atmospheric motion calculations (*viz*. diabatic heating, convection, etc.) that mainly depend on the direction of *w*.

Acknowledgements

Authors would like to acknowledge all the technical and scientific staffs of National Atmospheric Research Laboratory (NARL) and Research Institute of Sustainable Humanosphere (RISH), who directly or indirectly involved in the radar observations. Thanks to all the reanalyses data centres for providing the data through the portal of Research data archival (RDA) of NCEP/UCAR. One of the author KVS thank Indian Research Organisation for providing research associateship during this study. We sincerely thanks all the referees, Executive Editor and Editor for their constructive comments and suggestions.

Data availability: Analysed data (both radars and reanalyses) used in this study can be obtained on request. Raw time series data are available through open access in the following websites:

For Indian MST Radar : www.narl.gov.in

For EAR radar : www.rish-kyoto-u.ac.jp/ear/index-e.html

ERAi, ERA5, JRA-55 and NCEP/DOE-2 were downloaded from https://rda.ucar.edu and MERRA-2 from https://disc.gsfc.nasa.gov.in

Author's Contributions

Deleted: Our

Formatted: Font: Italic, Complex Script Font: Italic

Deleted: care

Deleted: This study provides the reanalysis community an initial basis to improve the methodology for calculating *w* in reanalysis, as this is a much sought-parameter for atmospheric circulation calculations and analysis.

Deleted: ¶

Deleted: ¶

Deleted: ¶

Deleted: three

Formatted: Default Paragraph Font, Font: (Default) +Body (Calibri), 11 pt, Complex Script Font: +Body CS (Mangal), 10 pt, English (U.S.)

Formatted: Default Paragraph Font, Font: (Default) +Body (Calibri), 11 pt, Complex Script Font: +Body CS (Mangal), 10 pt, English (U.S.)

Formatted: Default Paragraph Font, Font: (Default) +Body (Calibri), 11 pt, Complex Script Font: +Body CS (Mangal), 10 pt

Formatted: Default Paragraph Font, Font: (Default) +Body (Calibri), 11 pt, Complex Script Font: +Body CS (Mangal), 10 pt

Deleted: ¶

KNU conceived the idea for validation of vertical velocity among the reanalyses. SSD, MVR, and KVS collected and analysed the MST radar spectrum data. All the authors contribute for generation of figures, interpretation and manuscript preparation. The data used in the present study can be obtained on request.

Conflict of Interest

The authors declare that there is no conflict of interest.

References

Anandan, V.K., Reddy, G.R., Rao, P.B.: Spectral analysis of atmospheric signal using higher orders spectral estimation technique, IEEE Trans. Geosci. Remote Sens., 39, 1890. https://doi.org/10.1109/36.951079, 2001.

Arakawa, A., and Schubert, W.H.: Interaction of a cumulus cloud ensemble with the large-scale environment- Part I, J. Atmos. Sci., 31(3), 674-701, https://doi.org/10.1175/1520-0469 031<0674:IOACCE>2.0.CO;2, 1974.

Back, L. E., and Bretherton, C.S.: Geographic variability in the export of moist static energy and vertical motion profiles in the tropical Pacific, Geophys. Res. Lett., 33, L17810, https://doi.org/10.1029/2006GL026672, 2006.

Bechtold, P., Chaboureau, J.P., Beljaars, A., Betts, A.K., Köhler, M., Miller, M., and Redelsperger, J.L.: The simulation of the diurnal cycle of convective precipitation over land in a global model. Q. J. Roy. Met. Soc., 130 (604), 3119-3137, https://doi.org/10.1256/qj.03.103, 2004.

Bechtold, P., Koehler, M., Jung, T., Doblas Reyes, F., Leutbecher, M., Rodwell, M.J., Vitart, F., and Balsamo, G.: Advances in simulating atmospheric variability with the ECMWF model: From synoptic to decadal time-scales, Q. J. Roy. Met. Soc., 134 (634), 1337-1351, https://doi.org/10.1002/qj.289,2008.

Deleted: ¶

Deleted: ¶

Deleted: pp.

Deleted: -

Formatted: Font: (Default) Cambria Math, Complex Script Font: Cambria Math

Deleted: -

Deleted: pp.

Formatted: Font: (Default) Cambria Math, Complex Script Font: Cambria Math

Deleted: https://doi.

Briegle, B. P.: Longwave band model for thermal radiation in climate studies, J. Geophys. Res., 97, 11475-11485, https://doi.org/10.1029/92JD00806, 1992.

Campana, K. A., Hou, Y.T., Mitchell, K. E., Yang, S. K., and Cullather, R.: Improved diagnostic cloud parameterization in NMC's global model, Preprints, 10th Conf. on Numerical Weather Prediction, Portland, OR, Amer. Meteor. Soc., 324-325, 1994.

Chou, M.D.: A solar radiation model for use in climate studies., J. Atmos. Sci., 49, 762-772, https://doi.org/10.1175/1520-0469(1992)049<0762:ASRMFU>2.0.CO;2, 1992.

Chou, M. D., and Lee, K. T.: Parameterizations for the absorption of solar radiation by water vapor and ozone, J. Atmos. Sci., 53, 1203-1208, https://doi.org/10.1175/1520-0469(1996)053<1203:PFTAOS>2.0.CO;2, 1996.

Chou, M.D., and Suarez, M.J.: A Solar Radiation Parameterization (CLIRAD-SW) Developed at Goddard Climate and Radiation Branch for Atmospheric Studies, NASA Technical Memorandum NASA/TM-1999-104606, 1999.

Chou, M.D., Lee, K. T., and Yang, P.: Parameterization of shortwave cloud optical properties for a mixture of ice particle habits for use in atmospheric models, J. Geophys. Res., 107, 1-9, https://doi.org/10.1029/2002JD002061, 2001.

Damle, S. H., Chande, J. V., Heldar, S, Chakravarthy, T., Ray, K. P .: Proceedings of the V international workshop on technical and scientific aspects of MST radar, august, 6-9, Aberywth, UK, STEP Handbook, Ed. Belva Edwards, SCOSTEP secretariat, Illinois, USA, 1991.

Das, S. S., Uma, K. N., Bineesha, V. N., Suneeth, K. V., Ramkumar G.: Four decadal climatological intercomparison of rocketsonde and radiosonde with different reanalysis data: results from Thumba Equatorial Station, Q. J. Roy. Met. Soc., https://doi.org/10.1002/qj.2632, 2015.

Dee D. P et al.: The ERA-Interim reanalysis: Configuration and performance of the data assimilation system, Q. J. R. Meteorol. Soc., 137, 553–597, https://doi.org/10.1002/qj.828, 2011.

European Centre for Medium-Range Weather Forecasts. 2009, updated monthly. ERA-Interim Project. Research Data Archive at the National Center for Atmospheric Research, Computational and Information Systems Laboratory. https://doi.org/10.5065/D6CR5RD9, Accessed 17 July 2019 and 29 July 2020.

European Centre for Medium-Range Weather Forecasts. 2017, updated monthly. ERA5 Reanalysis. Research Data Archive at the National Center for Atmospheric Research, Computational and Information Systems Laboratory. https://doi.org/10.5065/D6X34W69. Accessed 24 Jun 2019 and 30 July 2020.

Farr, T. G., Rosen, P. A., Caro, E., Crippen, R., et al. : The shuttle radar topography mission, Rev. Geophys., 45(2), http://dx.doi.org/10.1029/2005RG000183, 2007.

Fouquart, Y., Buriez, J. C., Herman, M., Kandel, R. S.: The influence of clouds on radiation: A climate-modeling perspective, J. Geophys. Res., 28, 145-166, https:// doi.org/10.1029/RG028i002p00145, 1990.

Fukao, S., Hashiguchi, H., Yamamoto, M., Tsuda, T., Nakamura, T., Yamamoto, M. K., Sato, T., Hagio, M., and Yabugaki, Y.: Equatorial Atmosphere Radar (EAR): System description and first results, Radio Sci., 38(3), 1053, https://doi.org/10.1029/2002RS002767, 2003.

Fujiwara M, Jackson D.: SPARC Reanalysis Intercomparison Project (SRIP) planning meeting, 29 April–1 May 2013, Exeter, UK. SPARC Newsletter. 41: 52–55, 2013.

Fujiwara M, Polavarapu S, Jackson D.: A proposal of the SPARC reanalysis/analysis intercomparison project. SPARC Newsletter. 38: 14–17, 2013.

Deleted: Dowdy, A., R. A. Vincent, K. Igarashi, Y. Murayama and D.J. Murphy.: A comparison of mean winds and gravity wave activity in the northern and southern polar MLT. Geophy.Res.Lett., 28(8), 1475- 1478. https://doi.org/10.1029/2000GL012576, 2001¶

Deleted: .

Deleted: H.

Deleted: M.

Deleted: T.

Deleted: T.

Deleted: M. K.

Deleted: T.

Deleted: M.

Deleted: Y.

Deleted: ¶

Fujiwara, M., Wright, J. S., Manney, G. L., et al.: Introduction to the SPARC Reanalysis Intercomparison Project (S-RIP) and overview of the reanalysis systems, Atmos. Chem. Phys., 17, 1417–1452, https://doi.org/10.5194/acp-17-1417-2017, 2017.

Gage, K. S., McAfee, J. R., Collins, W. G., Söderman, D., Böttger, H., Radford, A., and Balsley, B.B.: A comparison of winds observed at Christmas Island using a wind-profiling Doppler radar with NMC and ECMWF analyses, Bull. Amer. Meteor. Soc. (1988) 69 (9): 1041–1046, https://doi.org/10.1175/1520-0477(1988)069<1041:ACOWOA>2.0.CO;2, 1988.

Gage, K. S., McAfee, J. R., Carter, D. A., Ecklund, W. L., Riddle, A. C., Reid, G. C., and Balsley, B.B.: Long-term mean vertical motion over the tropical Pacific: Wind-profiling Doppler radar measurements. Science, 254(5039), 1771-1773, https://doi.org/10.1126/science.254.5039.1771, 1991

Gage, K. S., McAfee, J. R., and Reid, G. C. (1992). Diurnal variation in vertical motion over the central equatorial Pacific from VHF wind-profiling Doppler radar observations at Christmas Island (2° N, 157° W). Geophy. Res. Lett., 19(18), 1827-1830,https://doi.org/10.1029/92GL02105, 1992

Gelaro, et al.: The Modern-Era Retrospective Analysis for Research and Applications, Version 2 (MERRA-2), J. Clim., 30, 5419-5454, https://doi.org/10.1175/JCLI-D-16-0758.1, 2017.

Hersbach, H. et al.: The ERA5 global reanalysis. Q. J. Roy. Met. Soc., https://doi.org/10.1002/qj.3803, 2020.

Holton, J.R.: An Introduction to Dynamic Meteorology, Academic Press, 3rd Ed, ISBN:9780123543554, 2004.

Hoffmann, L., Günther, G., Li, D., Stein, O., Wu, X., Griessbach, S., Heng, Y., Konopka, P., Müller, R., Vogel, B., and Wright, J. S.: From ERA-Interim to ERA5: the considerable

Deleted: https://doi.org/10.5194/acp-17-1417-2017

Formatted: Default Paragraph Font, Font: (Default) +Body (Calibri), 11 pt, Complex Script Font: +Body CS (Mangal), 10 pt

Formatted: Default Paragraph Font, Font: (Default) +Body (Calibri), 11 pt, Complex Script Font: +Body CS (Mangal), 10 pt

Formatted: Indent: Hanging: 0.25"

Deleted: &

Deleted: ¶

Deleted: &

Deleted: . B

Deleted: &

Deleted: sical research letters,

Formatted: Font: 12 pt, Complex Script Font: 12 pt

impact of ECMWF's next-generation reanalysis on Lagrangian transport simulations, Atmos. Chem. Phys., 19, 3097–3124, https://doi.org/10.5194/acp-19-3097-2019, 2019.

Huaman, M., and B. B. Balsley.: Long-term average vertical motions observed by VHF wind profilers: The effect of slight antenna pointing inaccuracies, J. Atmos. Oceanic Technol., 13, 560– 569, 1996.

Iacono, M.J., Delamere, J. S., Mlawer, E. J., Shephard, M.W., Clough, S. A., and Collins, W.D.: Radiative forcing by long-lived greenhouse gases: Calculations with the AER radiative transfer models, J. Geophys. Res., 113, 1-8, https://doi.org/10.1029/2008JD009944, 2008.

Japan Meteorological Agency/Japan. 2013, updated monthly. JRA-55: Japanese 55-year Reanalysis, Daily 3-Hourly and 6-Hourly Data. Research Data Archive at the National Center for Atmospheric Research, Computational and Information Systems Laboratory. https://doi.org/10.5065/D6HH6H41, Accessed 18 Jun 2019.

Kanamitsu , M., Ebisuzaki, W., Woollen, J., Yang, S. K., Hnilo, J. J., Fiorino, M., and Potter, G. L.: NCEP-DOE AMIP-II reanalysis (R-2). Bull. Am. Meteorol. Soc., 83: 1631–1643, https://doi.org/ 10.1175/BAMS-83-11-1631, 2002.

Kawai, H., and Inoue, T.: A Simple Parameterization Scheme for Subtropical Marine Stratocumulus, SOLA., 2, 017-020,https://doi:10.2151/sola.2006-005, 2006.

Kawatani, Y., Hamilton, K., Miyazaki, K., Fujiwara, M., and Anstey, J. A.: Representation of the tropical stratospheric zonal wind in global atmospheric reanalyses, Atmos. Chem. Phys., 16, 6681-6699, doi: 10.5194/acp-16-6681-2016, 2016.

Kennedy, A. D., Dong, X., and Xi, B.: Comparison of MERRA and NARR Reanalyses with the DOE ARM SGP Data, J. Clim., https://doi.org/10.1175/2011JCLI3978.1, 2012.

Kobayashi, S., et al.: The JRA-55 Reanalysis: General specifications and basic characteristics, J. Meteorol. Soc. Jp., 93, https://doi.org/10.2151/jmsj.2015-001, 2015.

Deleted: .

Deleted: W.

Deleted: J.

Deleted: S. K.

Deleted: J. J.

Deleted: M.

Deleted: G. L.

Deleted: .

Deleted: X.

Deleted: d

Deleted: B.

Formatted: Font: (Default) Times New Roman, 12 pt, Complex Script Font: Times New Roman, 12 pt

Koscielny, A. J., Doviak, R. J., and Zrnic, D. S.: An evaluation of the accuracy of some radar wind profiling techniques, J. Atmos. Ocen. Tech., 1(4), 309-320, https://doi.org/10.1175/1520-0426(1984)001<0309:AEOTAO>2.0.CO;2, 1984.

Liou, Y.C., and Chang., Y. J.: A Variational Multiple-Doppler Radar Three-Dimensional Wind Synthesis Method and Its Impacts on Thermodynamic Retrieval, Mon. Wea. Rev., 137:11, 3992- 4010, https://doi.org/10.1175/2009MWR2980.1, 2009.

Matejka, T.: Estimating the most steady frame of reference from Doppler radar data, J. Atmos. Oceanic Technol., 19, 1035-1048, 2002.

Mlawer, E. J., Steven J.T., Patrick D.B., Michael J.I., and Clough, S. A.: Radiative transfer for inhomogeneous atmospheres: RRTM, a validated correlated-k model for the longwave, J. Geophys. Res., 102, 16663-16682, https://doi.org/10.1029/97JD00237, 1997.

Modern-Era Retrospective Analysis for Research and Applications, Version 2 (MERRA-2), Research Data Archive at the NASA Goddard Earth Sciences data and information service centre (GES-DISC) .http://dx.doi.org/10.5067/QBZ6MG944HW0, Accessed 5 Jul 2019.

Molod, A., Takacs, L., Suarez, M., and Bacmeister, J.: Development of the GEOS-5 atmospheric general circulation model: evolution from MERRA to MERRA2, Geosci. Model Dev., 8, 1339-1356, https://doi:10.5194/gmd-8-1339-2015, 2015.

Moorthi, S., and Suarez, M.J.: Relaxed Arakawa-Schubert. A Parameterization of Moist Convection for General Circulation Models, Mon. Wea. Rev., 120 (6): 978–1002, https://doi.org/10.1175/1520-0493(1992)120<0978:RASAPO>2.0.CO;2, 1992.

Morcrette, J. J.: Radiation and cloud radiative properties in the European Centre for Medium Range Weather Forecasts forecasting system, J. Geophys. Res., 96, 9121-9132, https://doi.org/10.1029/89JD01597, 1991.

Deleted: ¶

Deleted: Laskar, F. I., et al.: Experimental evidence of arctic summer mesospheric upwelling and its connection to cold summer mesopause, Geophys. Res. Lett., 44, 9151- 9158. https://doi.org/10.1002/2017GL074759, 2017¶

Formatted: Font: (Default) Times New Roman, 12 pt, Complex Script Font: Times New Roman, 12 pt

Deleted: .

Deleted:).

Deleted:

Formatted: Default Paragraph Font, Font: (Default) +Body (Calibri), 11 pt, Complex Script Font: +Body CS (Mangal), 10 pt

Muschinski, A.: Possible effect of Kelvin-Helmholtz instability on VHF radar observations of the mean vertical wind, J. Appl. Meteorol., 35, 2210–2217, https://doi.org/10.1175/1520-0450(1996)035<2210:PEOKHI>2.0.CO;2, 1996.

Nastrom, G. D., and VanZandt, T. E.: Mean vertical motions seen by radar wind profilers, J. Appl. Meteorol., 33, 984–995, https://doi.org/10.1175/1520-0450(1994)033< 0984:MVMSBR>2.0.CO;2 , 1994.

National Centers for Environmental Prediction/National Weather Service/NOAA/U.S. Department of Commerce. 2000. NCEP/DOE Reanalysis 2 (R2). Research Data Archive at the National Center for Atmospheric Research, Computational and Information Systems Laboratory. https://doi.org/10.5065/KVQZ-YJ93, Accessed 7 Jan 2019.

Peterson, V. L., and Balsley, B. B.: Clear air Doppler measurements of the vertical component of wind velocity in the troposphere and stratosphere. Geophys. Res. Lett., 6(12), https://doi.org/10.1029/GL006i012p00933, 1979,

Rao, P. B., Jain, A. R., Kishore, P., Balamuralidhar, P., Damle, S. H., and Viswanathan, G.: Indian MST radar 1. System description and sample vector wind measurements using ST mode, Radio Sci., 30, 1125–1138, https://doi.org/10.1029/95RS00787, 1995.

Rao, T.N, Uma, K. N., Rao, D. N., and Fukao, S.: Understanding the transportation process of tropospheric air entering the stratosphere from direct vertical air motion measurements over Gadanki and Kototabang, Geophys. Res. Lett., 35, L15805, https://doi.org/10.1029/2008GL034220, 2008.

Rao, T. N., Uma, K. N, Satyanarayana, T. M., and Rao, D. N.: Differences in Draft Core Statistics from the Wet to Dry Spell over Gadanki, India (13.5°N, 79.2°E), Mon.Wea.Rev, 137, 4293-4306, https://doi.org/10.1175/2009MWR3057.1, 2009.

Rao, V., Rao, D. N., Ratnam, M. V., Mohan, K., and Rao, S.: Mean Vertical Velocities Measured by Indian MST Radar and Comparison with Indirectly Computed Values, J.

Formatted: Font: (Default) Times New Roman, 12 pt, Complex Script Font: Times New Roman, 12 pt

Deleted: doi

Formatted: Font: (Default) Times New Roman, 12 pt, Complex Script Font: Times New Roman, 12 pt

Formatted: Font: (Default) Times New Roman, 12 pt, Complex Script Font: Times New Roman, 12 pt

Deleted: T. E.

Deleted: .

Deleted: B. B.

Deleted: A. R.

Deleted: P.

Deleted: P.

Deleted: S. H.

Deleted: G.

Formatted: Default Paragraph Font, Font: (Default) +Body (Calibri), 11 pt, Complex Script Font: +Body CS (Mangal), 10 pt

Deleted: K. N.

Deleted: ,

Deleted: D. Narayana

Deleted: S.

Deleted: T. M.

Deleted: D. N.

Deleted: D.

Deleted: M. V.

Deleted: K.

Deleted:

Deleted: S.

App. Meteo, 42(4), 541-552, https://doi.org/10.1175/1520-0450(2003)042<0541:MVVMBI>2.0.CO;2, 2003.

Röttger, J.: Reflection and scattering of VHF radar signals from atmospheric refractivity structures, Radio Sci.,15, 259-276, https://doi.org/10.1029/RS015i002p00259, 1980.

Stepanyuk, O., Jouni, R., Sinclair, V.A., and Järvinen, H.: Factors affecting atmospheric vertical motions as analyzed with a generalized omega equation and the OpenIFS model. Tellus., 69. 1271563. https://doi.org/10.1080/16000870.2016.1271563, 2017.

Schumann, U.: The horizontal spectrum of vertical velocities near the tropopausefrom global to gravity wave scales. J. Atmos. Sci., 76, 3847-3862, https://doi.org/10.1175/JAS-D-19-0160.1, 2019

Tanaka, H. L., and Yatagai, A.: Comparative study of vertical motions in the global atmosphere evaluated by various kinematic schemes, J. Meteo.Soc.Jp., 78, 289-298, 2000.

Tiedtke., M.: A Comprehensive Mass Flux Scheme for Cumulus Parameterization in Large-Scale Models, Mon. Wea. Rev., 117 (8): 1779–1800, https://doi.org/10.1175/1520-0493(1989)117<1779:ACMFSF>2.0.CO;2, 1989.

Uma, K. N., and Rao, T. N.: Characteristics of Vertical Velocity Cores in Different Convective Systems Observed over Gadanki, India, Mon.Wea.Rev., 137, 954-974, https://doi.org/10.1175/2008MWR2677.1, 2009a.

Uma, K. N., and Rao, T. N.: Diurnal variation in vertical air motion over a tropical station, Gadanki (13.5^{o}N, 79.2^{o}E), and its effect on the estimation of mean vertical air motion, J. Geophys. Res., 114, D20106, https://doi.org/10.1029/2009JD012560, 2009b.

Uma, K. N., Kumar, K. K., Das, S.S., Rao, T. N., and Satyanarayana, T. M.: On the Vertical Distribution of Mean Vertical Velocities in the Convective Regions during the Wet and

Formatted: Font: (Default) Times New Roman, 12 pt, Complex Script Font: Times New Roman, 12 pt

Deleted: doi ………………………………..,

Formatted: Font: (Default) Times New Roman, 12 pt, Complex Script Font: Times New Roman, 12 pt

Deleted: R.

Deleted: V.

Deleted: Heikki, ,

Deleted: ,

Deleted: A.

Dry Spells of the Monsoon over Gadanki, Mon. Weather Rev., 140, 398–410, https://doi.org/10.1175/MWR-D-11-00044.1, 2011.

Viswanathan, G., Kishore, P., Rao, P. B., Jain, A. R., Aravindhan, R., Balamuralidhar, P., and Damle, S. H.: Preliminary results using ST mode of the Indian MST radar: Measurment of vertical velocity, Ind. J. Rad. Sp. Phys., 22, 97-102, 1993.

Wang, J., Bian, J., Brown, W. O., Cole, H., Grubisic, V., and Young, K.: Vertical air motion from T-REX radiosonde and dropsonde data, J. Atmos. Oce. Tech., 26, 928-942, https://doi.org/10.1175/2008JTECHA1240.1, 2009.

Yamamoto, M. K., Nishi, N., Horinouchi, T., Niwano, M., and Fukao, S.: Vertical wind observation in the tropical upper troposphere by VHF wind profiler: A case study, Rad, Sci., 42, RS3005, https://doi.org/10.1029/2006RS003538, 2007.

Yamamoto, M. K., Fujiwara, M., Horinouchi, T. Hashiguchi, H., and Fukao, S.: Kelvin-Helmholtz instability around the tropical tropopause observed with the Equatorial Atmosphere Radar, Geophys. Res. Lett., 30(9), 1476, https://doi.org/10.1029/2002GL016685, 2003.

Zhang, J., Chen, H., Zhu, Y., Shi,H., Zheng, Y., Xia, X., Teng, Y., Wang, F., Han, X., Li, J., and Xuan, Y.: 2019, A novel method for estimating the vertical velocity of air with a descending radiosonde system, Rem. Sens., 11, 1538, https://doi.org/10.3390/rs11131538, 2019.

Deleted: P. …ishore, P., P.B.
Formatted
Deleted: A. R. …ain, A. R., R.
Formatted: Font: Not Bold, Complex Script Font: Not Bold
Formatted: Indent: Left: 0", Hanging: 0.25", Line spacing: Double
Formatted: Font: Not Bold, Complex Script Font: Not Bold
Deleted: P.
Formatted
Deleted: S. H.
Formatted: Font: Not Bold, Complex Script Font: Not Bold
Deleted: a
Deleted: J. …ian, J., W. O.
Formatted: Font: Not Bold, Complex Script Font: Not Bold
Deleted: H.
Deleted: …H., V.
Formatted: Font: Not Bold, Complex Script Font: Not Bold
Deleted:
Formatted: Font: Not Bold, Complex Script Font: Not Bold
Deleted: K.
Formatted: Font: Not Bold, Complex Script Font: Not Bold
Formatted: Font: Not Bold, Complex Script Font: Not Bold
Deleted: a
Formatted: Font: Not Bold, Complex Script Font: Not Bold
Deleted: https://doi:
Formatted
Deleted: ¶
Deleted: N. …ishi, N., T …orinouchi, T., M
Deleted: M. …ujiwara, M., T. …orinouchi, T.
Deleted: H. …hen, H., Y. …Zhu, Y., H.
Deleted: https://doi:

Figure captions

Figure 1. Topographical maps of the (a) IMSTR, and (b) Kototabang EAR sites in MSL, generated by using the Shuttle Radar Topography Mission (SRTM) data (Farr et al., 2007). Dots in the map indicate the radar locations.

Figure 2. Intercomparison of layer averaged daily *w* (12 UTC) measured from IMSTR with different reanalyses (ERAi, ERA5, MERRA-2, NCEP/DOE-2, and JRA-55) (12 UTC) over Gadanki for (a) January 2007, and (b) August 2007.

Figure 3. Same as Fig.2, but for EAR over Kototabang. Please note that for EAR, *w* is diurnal mean (24 hrs mean) for both EAR and reanalyses for (a) January 2008, and (b) August 2008.

Figure 4. Climatological monthly mean altitude profile of *w* obtained from IMSTR and 5-reanalysis over Gadanki from 1995-2015. Horizontal lines indicate the standard error.

Figure 5. Same as Fig.4, but over Kototabang from 2001 to 2015.

Figure 6. Monthly mean *w* obtained from (a) IMSTR and (b) ERAi for 5 years interval (from top to bottom) over Gadanki (12 UTC).

Figure 7. Same as Fig.6 but for diurnal mean over Kototabang.

Figure 8. Height profile of *w* at 12 UTC and diurnal mean (with 1 hour resolution) over Gadanki extracted from ERA5 during 1995-2015 (highest available time resolution).

Figure 9. Same as Fig.8 but for Kototabang during 2001-2015.

Figure10. Comparison of relative differences in *w* between the reanalysis ensemble mean and each reanalysis for Gadanki from 1995 to 2015. Individual month differences are estimated and then averaged for each month.

Deleted: ¶ ¶ ¶ ¶ ¶ ¶ ¶ ¶ ¶ ¶ ¶ ¶ ¶ ¶
Deleted: Gadanki MST radar
Formatted: Font: Not Italic, Complex Script Font: Not Italic
Deleted: i
Deleted: MST Radar
Deleted: Kototabang
Deleted: MST Radar
Formatted: Font: (Default) Times New Roman, 12 pt, Complex Script Font: Times New Roman, 12 pt
Deleted: MST Radar
Deleted: GMT
Deleted: GMT
Deleted: reanalysis for Gadanki

Figure 11. Same as Fig.10, but for Kototabang from 2001 to 2015.

Figure 12. (a) Map for spatial averaging (grid resolution), and height profiles of *w* for different spatial averaging at 00, 06, 12, and 18 UTC respectively for ERAi reanalysis during 2007.

Figure 13. Comparison of directional tendency of *w* between the radars and various reanalysis data sets for (a) Gadanki (1995-2015) and (b) Kototabang (2001-2015). Updrafts are shown in top and third panels and downdrafts are shown in middle and bottom panels (for details see text).

Figure S1 : Monthly mean climatology of *w* obtained from (a) radars, (b) ERAi, (c) ERA5, (d) MERRA-2, (e) NCEP/DOE-2, and JRA-55 over Gadanki (left) (1995-2015) and Kototabang (right) (2001-2015). Gadanki data are at 12 UTC and Kototabang data are diurnal mean.

Table captions

Table 1. The radar specifications and parameters used for the present measurements.

Table 2. Schemes of different reanalyses data used in the present study.

Figure 1. Topographical maps of the (a) Gadanki IMSTR, and (b) Kototabang EA radar sites in MSL, generated by using the Shuttle Radar Topography Mission (SRTM) data (*Farr et al.*, 2007). Dots in the map indicate the radar locations.

Deleted: MST radar

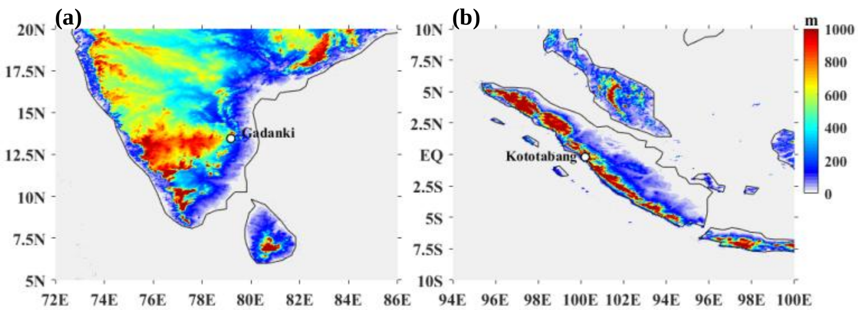

Figure 2. Intercomparision of layer averaged daily *w* (12 UTC) measured from JMSTR with different reanalyses (ERAi, ERA5, MERRA-2, NCEP/DOE-2, and JRA-55) (12 UTC) over Gadanki for (a) January 2007, and (b) August 2007.

Deleted: MST Radar

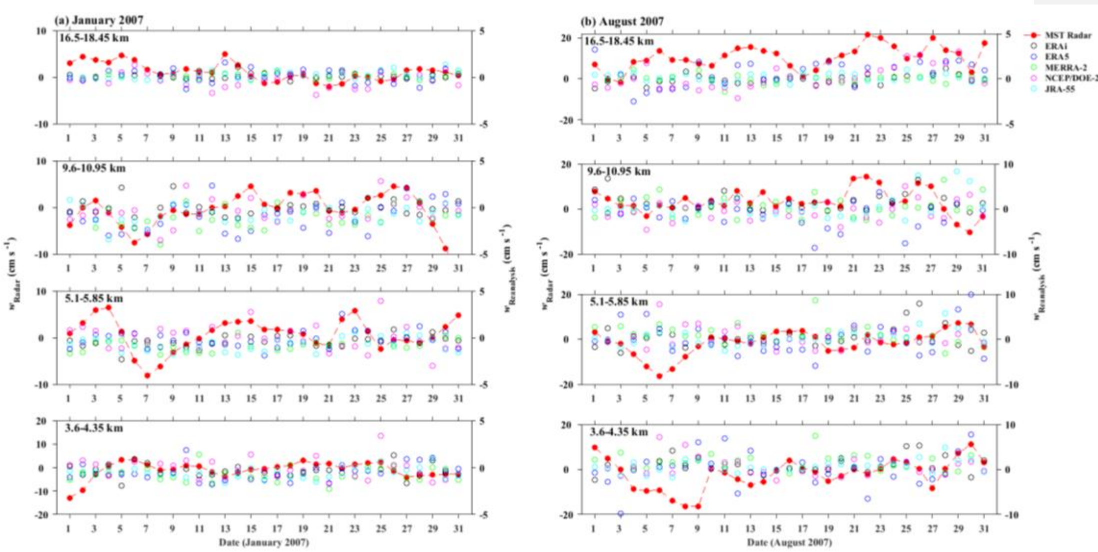

Figure 3. Same as Fig.2, but for EAR over Kototabang. Please note that for EAR, *w* is diurnal mean (24 hrs mean) for both EA radar and reanalyses for (a) January 2008, and (b) August 2008.

Deleted: for

Deleted: Kototabang

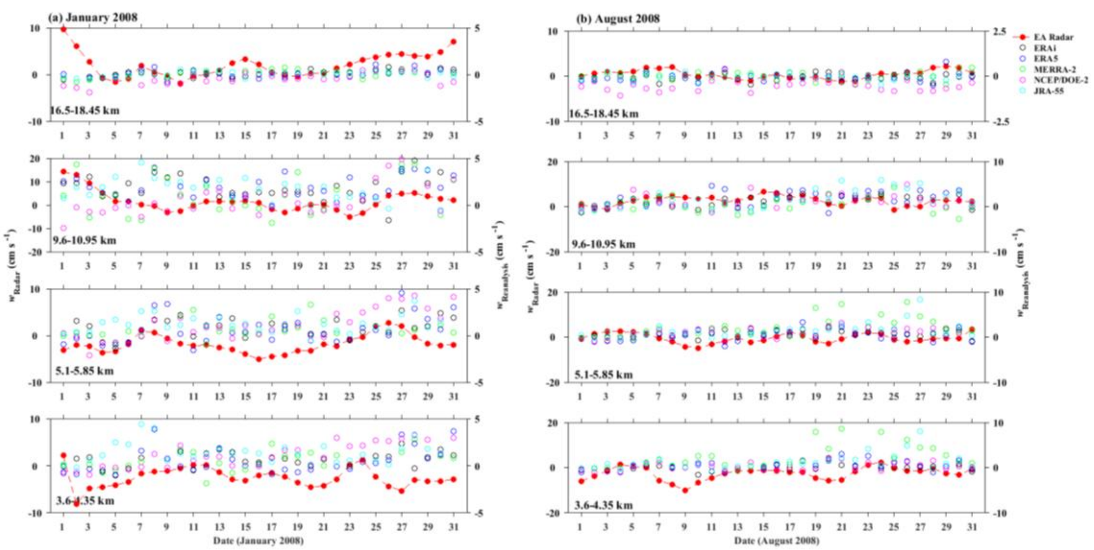

Figure 4. Climatological monthly mean altitude profile of *w* obtained from IMSTR and 5-reanalysis over Gadanki from 1995-2015. Horizontal lines indicate the standard error.

Deleted: MST Radar

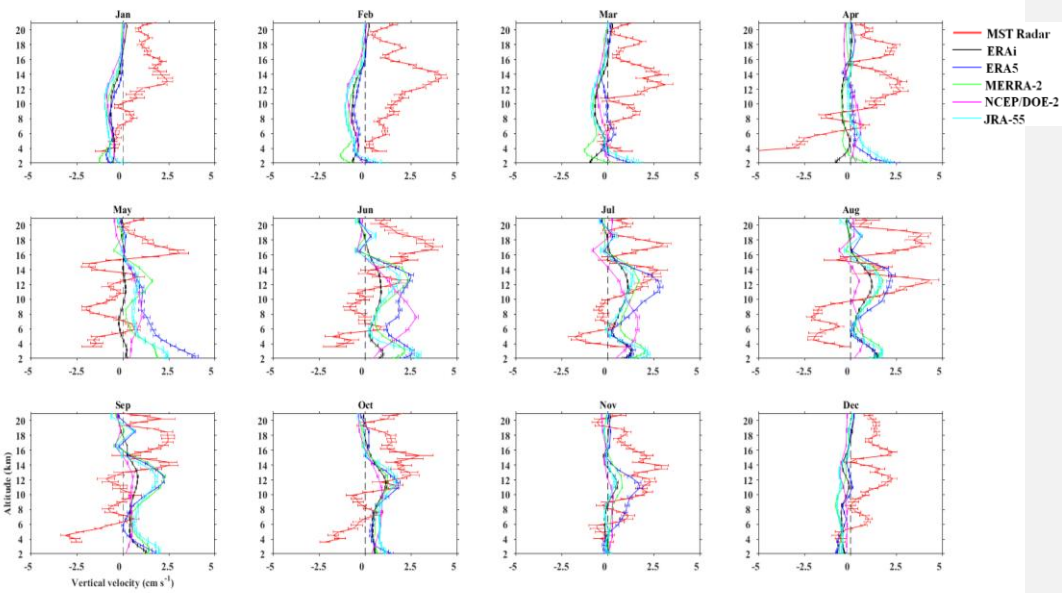

Figure 5. Same as Fig.4, but from EAR over Kototabang from 2001 to 2015.

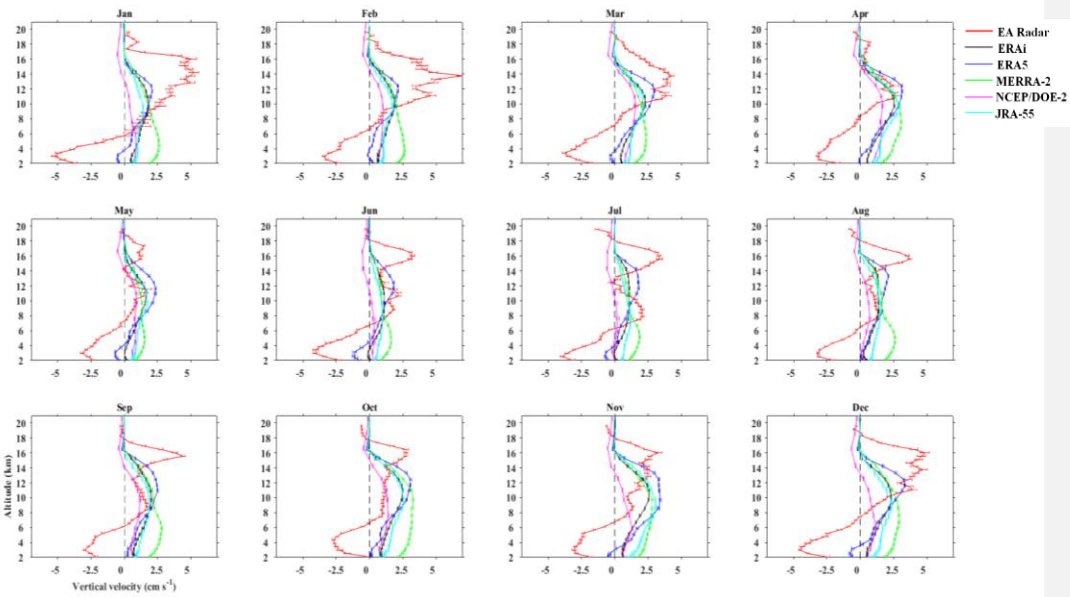

Figure 6. Monthly mean *w* obtained from (a) IMSTR and (b) ERAi for 5 years interval (from top to bottom) over Gadanki (12 GMT).

Deleted: MST Radar

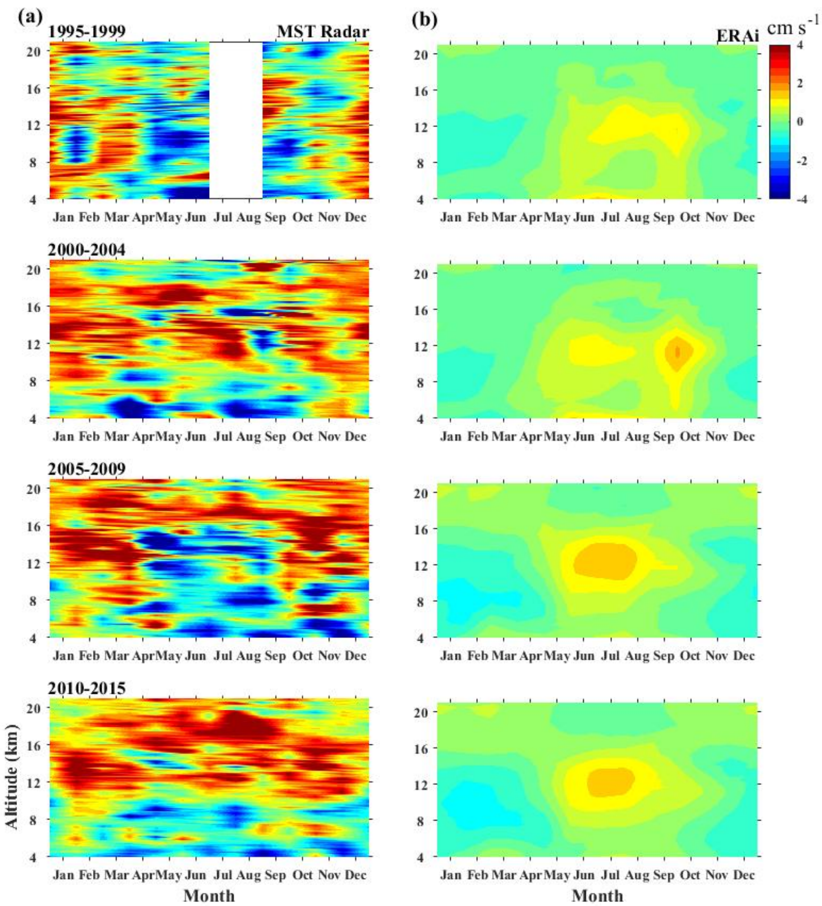

Figure 7. Same as Fig.6 but for diurnal mean from EAR over Kototabang.

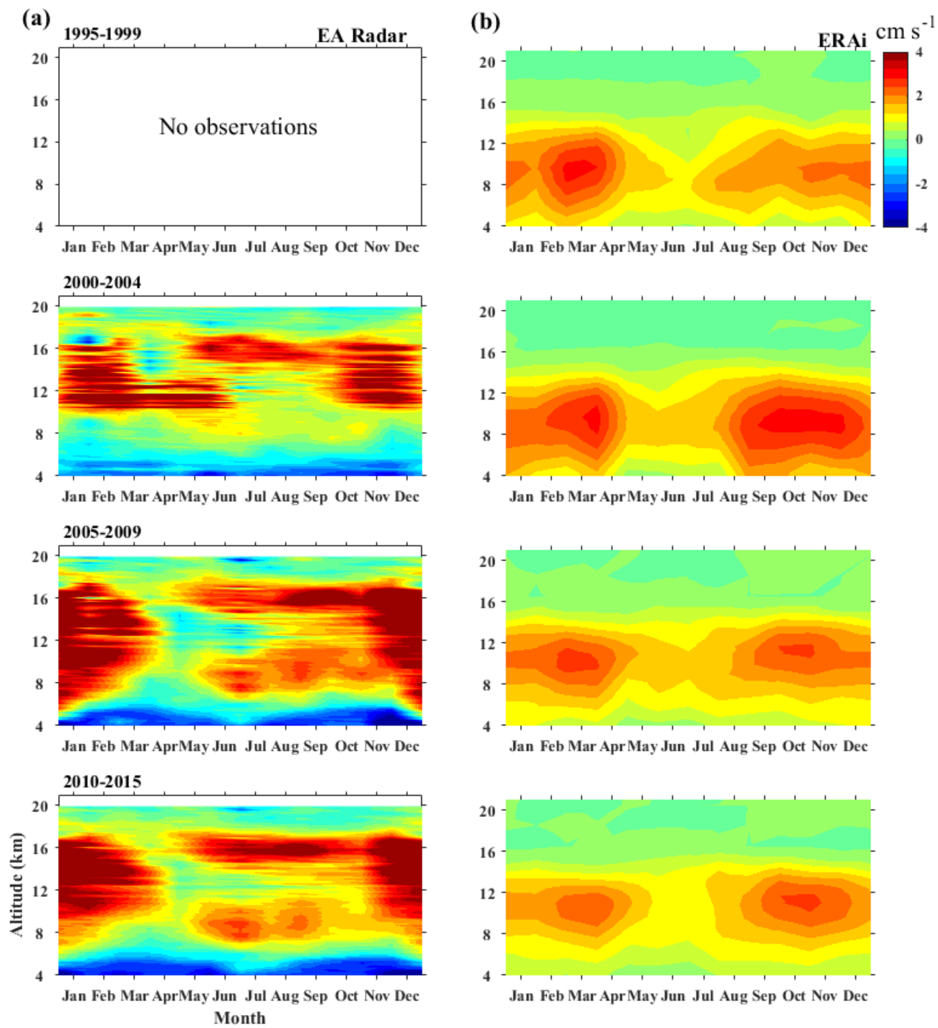

Figure 8. Height profile of *w* at 12 GMT and diurnal mean (with 1 hour resolution) over Gadanki extracted from ERA5 during 1995-2015 (highest available time resolution).

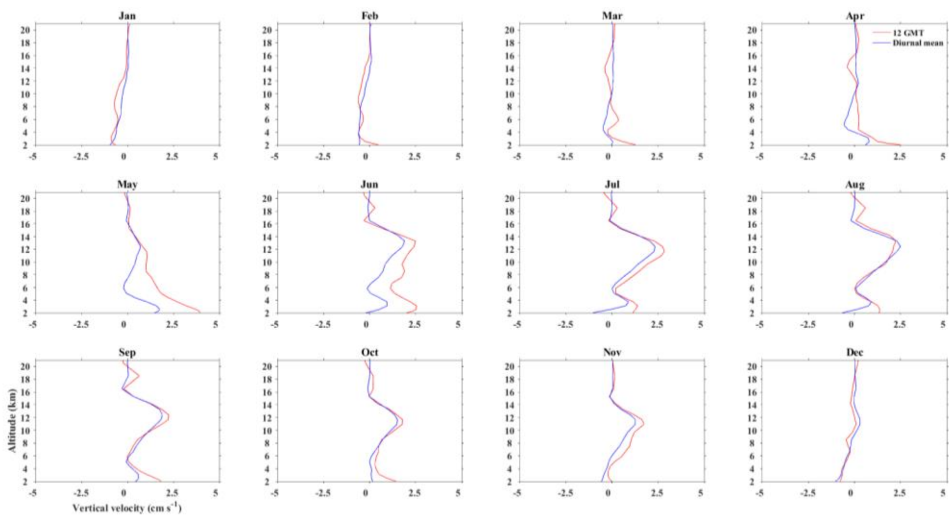

Figure 9. Same as Fig.8 but over Kototabang during 2001-2015.

Deleted: for

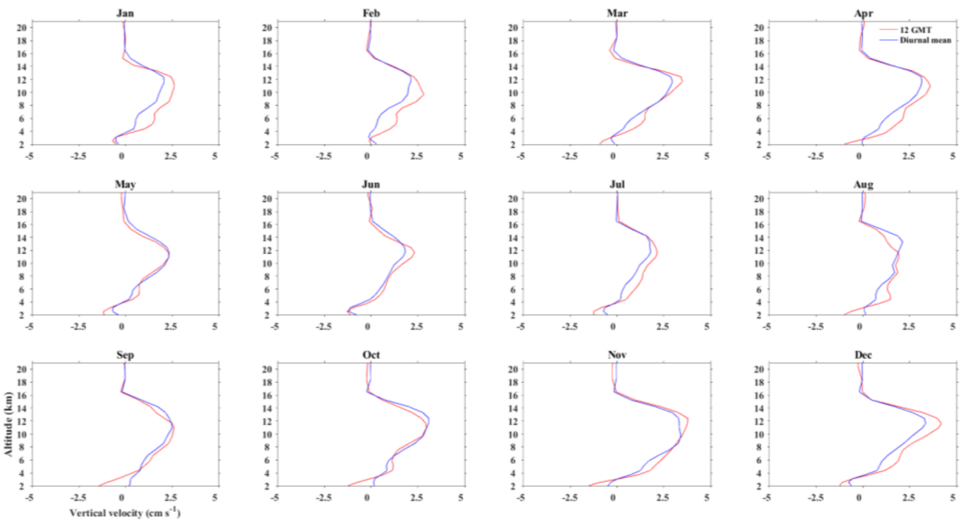

Figure10. Comparison of differences in *w* between the reanalysis ensemble mean and each reanalysis for Gadanki from 1995 to 2015. Individual month differences are estimated and then averaged for each month.

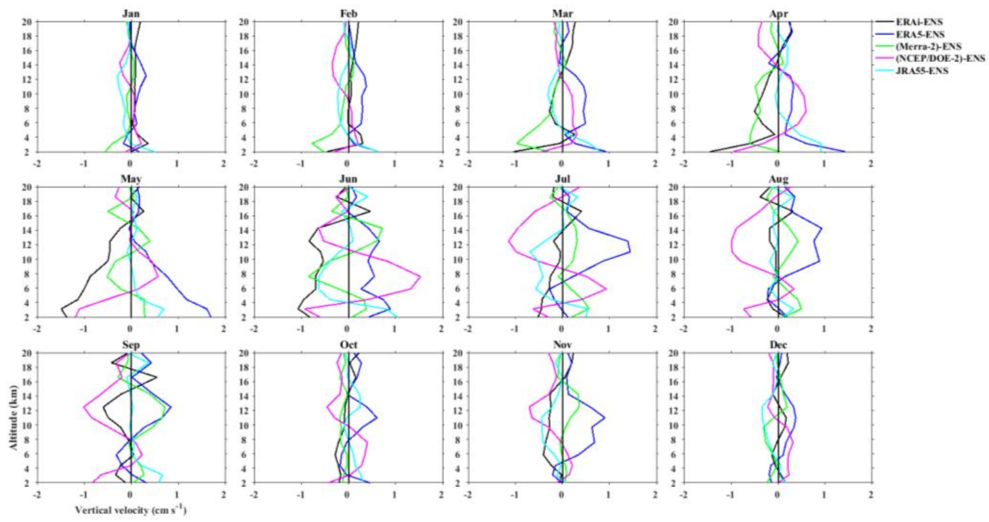

Deleted: relative

Deleted: reanalysis

Figure 11. Same as Fig.10, but for Kototabang from 2001 to 2015.

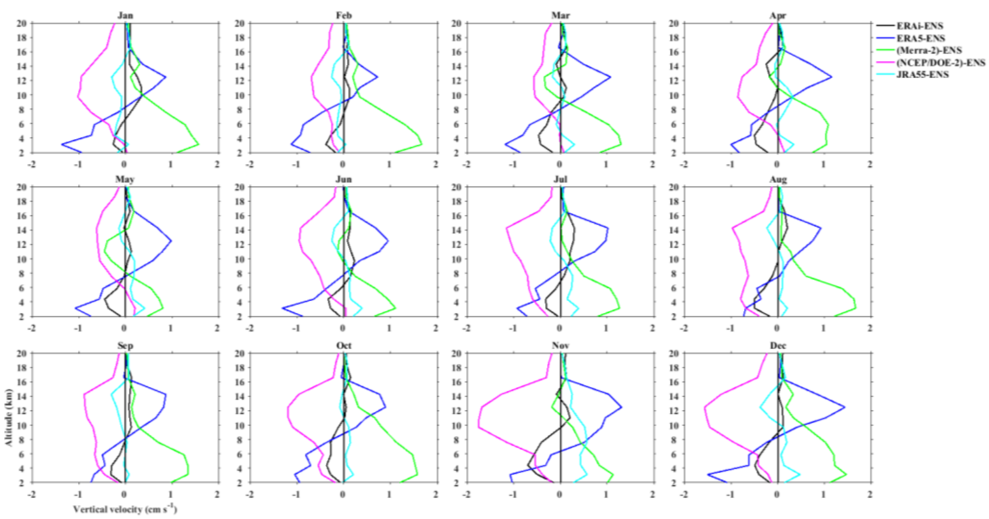

Figure 12. (a) Map for spatial averaging (grid resolution), and height profiles of *w* for different spatial averaging at 00, 06, 12, and 18 UTC for ERAi reanalysis during 2007.

Deleted: respectively

Deleted: 7 for ERAi reanlysis

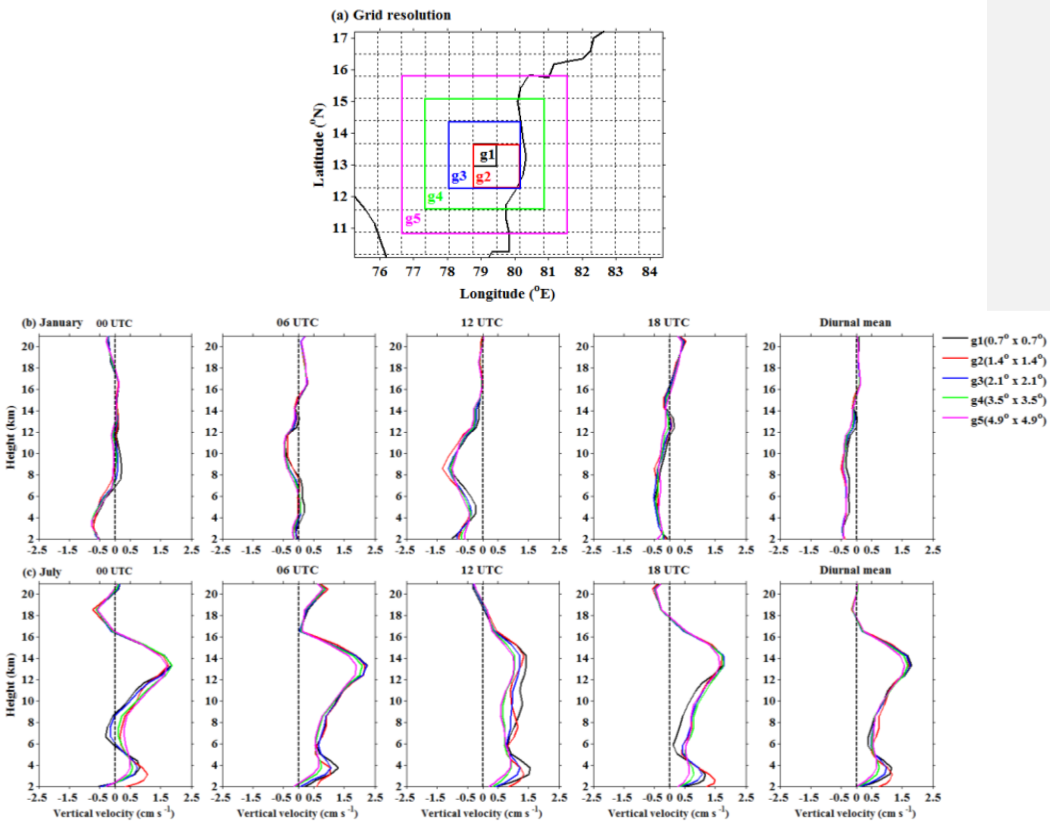

Figure 13. Comparison of directional tendency of *w* between the radars and various reanalysis data sets for (a) Gadanki (1995-2015) and (b) Kototabang (2001-2015). Updrafts are shown in top and third panels and downdrafts are shown in middle and bottom panels (for details see text).

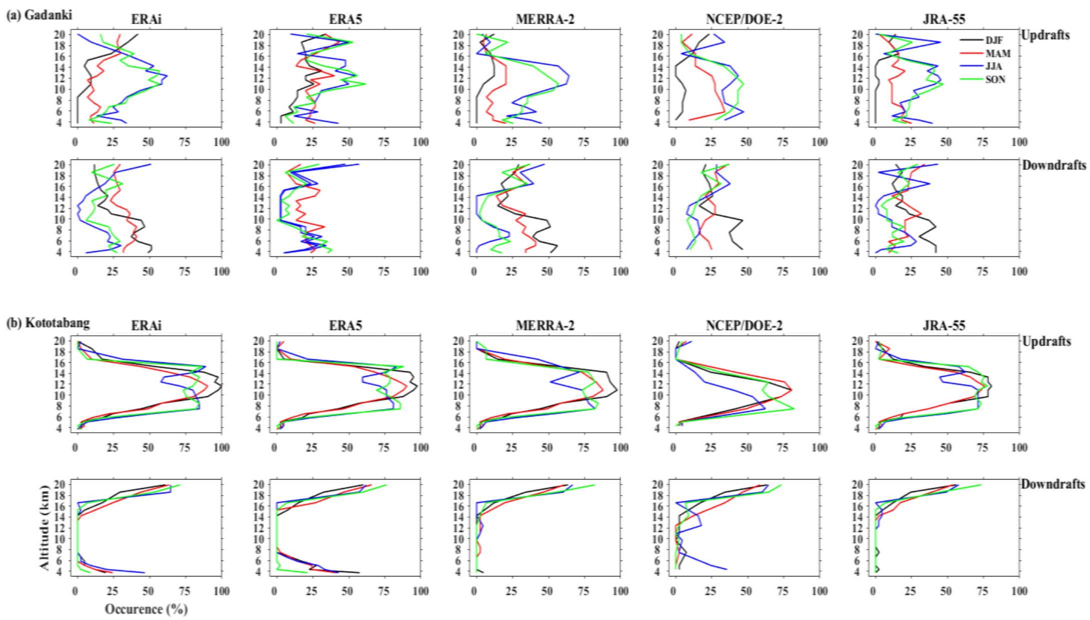

Figure S1 : Monthly mean climatology of *w* obtained from (a) radars, (b) ERAi, (c) ERA5, (d) MERRA-2, (e) NCEP/DOE-2, and JRA-55 over Gadanki (left) (1995-2015) and Kototabang (2001-2015) (right). Gadanki data are at 12 GMT and Kototabang data are diurnal mean.

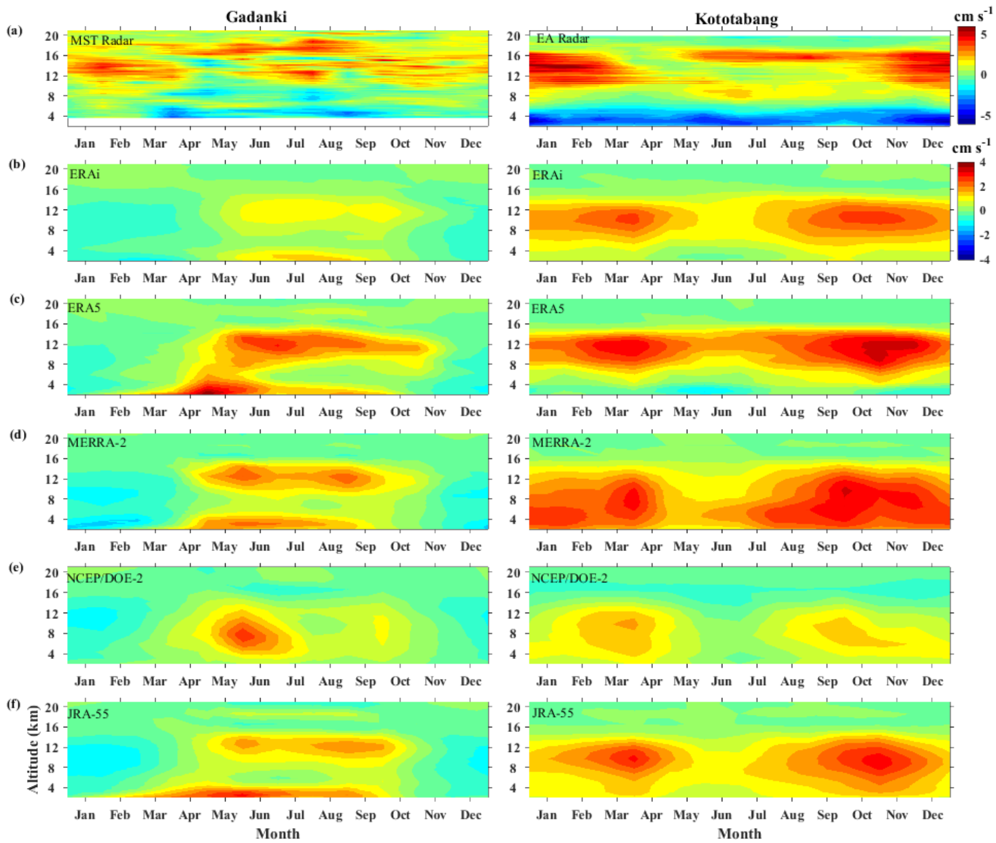

Table 1. The radars specifications and parameters used for the present measurements.

Parameter	**IMSTR**	**EAR**
Frequency	53 MHz	47 MHz
Peak power	2.5 MW	100 kW
Maximum duty cycle	2.5 %	5 %
Antenna	1024, three-element Yagi antennas	560, three-element Yagi antennas
Beam width	3 degree	3.4 degree
Mode of operation		
Pulse width	16 μs with complimentary with 1 μs baud	0.5 to 256 μs
Inter pulse period (IPP)	1000 μs	200 and 400 μs
Range Resolution	150 m	150 m
No. of FFT point (NFFT)	256	256, 512
No of coherent integration (NCI)	64, 128, 256, and 512	16 and 32
No. of Incoherent integration	1	5 and 7
No. of beam	6 10-degree off-zenith in East, West, North and South along with two orthogonal in zenith beams	5 10-degree off-zenith in East, West, North and South along with one zenith beams
Velocity resolution	0.03 ms^{-1} (CI=64, NFFT=256, IPP=1000 μs) 0.002 ms^{-1} (CI=512, NFFT=256, IPP=1000 μs)	0.002 ms^{-1} (CI=32, NFFT=512, IPP=400 μs) 0.005 ms^{-1} (CI=16, NFFT=256, IPP=200 μs)
Data format	Spectrum	Spectrum

Formatted Table

Formatted: Font: (Default) Times New Roman, Complex Script Font: Times New Roman, (Complex) Arabic (Saudi Arabia), Superscript

Table 2. Schemes of different reanalyses data used in the present study.

Description	**ERA-Interim**	**ERA5**	**MERRA2**	**JRA55**	**NCEP2**
Spatial Resolution	0.75^{o} x 0.75^{o}	0.28^{o} x 0.28^{o}	0.5^{o} x 0.65^{o}	1.25^{o} x 1.25^{o}	2.5^{o} x 2.5^{o}
Longwave	*Mlawer et al* (1997)	*Morchrette* (1991)	*Chou et al* (2001)	*Chou et al* (2001)	*Mlawer et al.* (1997)
Shortwave	*Fouquart and Bonnel* (1990)	*Iacono et al* (2008)	*Chou and Suarez* (1999)	*Briegleb* (1992)	*Chou*. (1992); *Chou and Lee* (1996)
Convective Parametrization	*Tiedtke* (1989)	Convective mass flux scheme *Tidkete* (1989)	Relaxed Arakawa-Schubert (RAS, *Moorthi and Suarez* (1992)	Prognostic Arakawa-Schubert with DCAPE	Simplified *Arakawa Schubert scheme* (1974)
Cloud Scheme	*Bechtold et al*., (2004)	*Bechtold et al* (2008)	*Molod et al.* (2015).	*Kawai and Inoue* (2006)	*Campana et al.* (1994)
Data Assimilation	4D var	4D var	3D var with IAU	4-D var	3D VAR
References	*Dee et al* (2011)	*Hersbach et al* (2020)	*Gelaro et al* (2017)	*Kobayashi et al* (2015)	*Kanamitsu et al* (2002)
Vertical levels	L60	L137	L72	L40	L28

Deleted: ,
Deleted: ,
Deleted: ,
Deleted: ,
Deleted: ,
Deleted: ,
Deleted: ,
Deleted: ,
Deleted: ,
Deleted: ,
Deleted: ,
Deleted: ,
Deleted: ,
Deleted: ,
Deleted: ,
Deleted:
Deleted: ,
Deleted: ,
Deleted: ,
Deleted: ,
Deleted: ,
Deleted: *Kobayachi*
Deleted: ,
Deleted: ,
Deleted: ,
Deleted: ,